

**MODELLING AND SIMULATION OF PROTON  
EXCHANGE MEMBRANE FUEL CELL USING  
MATLAB/SIMULINK**



**2017  
M. Sc. Thesis  
Electrical-Electronics Engineering**

**MUNER A. ABDALRAZG KHAIRALLA**

**MODELLING AND SIMULATION OF PROTON EXCHANGE MEMBRANE  
FUEL CELL USING MATLAB/SIMULINK**

**A THESIS SUBMITTED TO  
THE GRADUATE SCHOOL OF NATURAL AND APPLIED SCIENCES OF  
KARABUK UNIVERSITY**

**BY**

**Muner A. Abdalrazg KHAIRALLA**

**IN PARTIAL FULFILLMENT OF THE REQUIREMENTS FOR  
THE DEGREE OF MASTER OF SCIENCE IN  
DEPARTMENT OF  
ELECTRICAL-ELECTRONICS ENGINEERING**

**December 2017**

I certify that in my opinion the thesis submitted by Muner A. Abdalrazg KHAIRALLA titled "MODELLING AND SIMULATION OF PROTON EXCHANGE MEMBRANE FUEL CELL USING MATLAB/SIMULINK" is fully adequate in scope and in quality as a thesis for degree of Master of Science.

Assoc. Prof. Dr. Ziyodulla YUSUPOV

Thesis Advisor, Department of Electrical-Electronics Engineering




This thesis is accepted by the examining committee with a unanimous vote in the Department of Electrical-Electronics Engineering as master thesis. December 7, 2017

Examining Committee Members (Institutions)

Signature

Chairman : Assist. Prof. Dr. Hüseyin ALTINKAYA (KBU)



Member : Assoc. Prof. Dr. Ziyodulla YUSUPOV (KBU)



Member : Assist. Prof. Dr. Metin VARAN (SAU)



22/12/2017

The degree of Master of Science by the thesis submitted is approved by the Administrative Board of the Graduate School of Natural and Applied Sciences, Karabuk University.

Prof. Dr. Filiz ERSÖZ

Head of Graduate School of Natural and Applied Sciences





*“I declare that all the information within this thesis has been gathered and presented in accordance with academic regulations and ethical principles and I have according to the requirements of these regulations and principles cited all those which do not originate in this work as well.”*

Muner A. Abdalrazg Khairalla

## **ABSTRACT**

**M. Sc. Thesis**

### **MODELLING AND SIMULATION OF PROTON EXCHANGE MEMBRANE FUEL CELL USING MATLAB/SIMULINK**

**Muner A. Abdalrazg KHAIRALLA**

**Karabuk University**

**Graduate School of Natural and Applied Sciences**

**Department of Electrical-Electronics**

**Thesis Advisor:**

**Assoc. Prof. Dr. Ziyodulla YUSUPOV**

**December 2017, 67 pages**

Last decades with rapidly integration of distributed energy resources to the power system, the interest on microgrid is growing. Microgrid is a basic element and a key component of Smart Grid. Microgrid combines distributed energy resources, such as PV, wind, microturbines, fuel cells, combined heat and power, storage devices (flywheels, energy capacitors and batteries) and flexible loads, and connected to the power grid via switches. Microgrid is intended to improve the energy efficiency, reliability of power system and decrease carbon dioxide emissions.

Proton Exchange Membrane Fuel Cell as one of the type of fuel cells is investigated in this thesis. PEM Fuel Cell has an improved performance with its fast start up time and low operating temperature than another type of fuel cells .Dynamic model of proton exchange membrane fuel cell is developed on MATLAB/Simulink. The

equivalent electrical circuits with their properties, the thermodynamic property of the fuel cell and the double-layer charging effect are used for modeling of fuel cell system. This model could expect the electrical response of the PEM fuel-cell stack under steady-state as well as transient conditions. Also, this model could be estimate the temperature response of the fuel-cell stack and show the potential to be useful in external controller design applications for Proton exchange membrane fuel cells.

**Key Words** : Distributed energy resources, microgrid, proton exchange membrane fuel cell, MATLAB/Simulink.

**Science Code** : 905.1.17

## ÖZET

**Yüksek Lisans Tezi**

### **MATLAB/SIMULINK İLE PROTON DEĞİŞİMLİ MEMBRAN YAKIT HÜCRELERİNİN MODELLENMESİ VE SİMÜLASYONU**

**Muner A. Abdalrazg KHAIRALLA**

**Karabük Üniversitesi**

**Fen Bilimleri Enstitüsü**

**Elektrik-Elektronik Mühendisliği Anabilim Dalı**

**Tez Danışmanı:**

**Doç. Dr. Ziyodulla YUSUPOV**

**Aralık 2017, 67 sayfa**

Dağıtık enerji kaynaklarının güç sistemine hızla entegrasyonu ile son on yıllarda, mikro şebekelere olan ilgi artmaktadır. Mikro şebeke, Akıllı Şebekenin temel bir unsuru ve ana bileşenidir. Mikro şebeke, PV, rüzgar, mikro türbinler, yakıt hücreleri, kombine ısı ve güç, depolama aygıtları (volan, enerji kapasitörü ve batarya) ve esnek yükler gibi dağıtık enerji kaynaklarını birleştirir ve anahtarlar vasıtasıyla elektrik şebekesine bağlanır. Mikro şebeke, enerji verimliliğini artırmak, güç sisteminin güvenilirliğini ve karbon dioksit emisyonlarını azaltmak için tasarlanmıştır.

Bu tezde yakıt hücrelerinden biri olan Proton Değişimli Membran (PDM) Yakıt Hücresi araştırılmıştır. PDM Yakıt Pili, hızlı başlatma süresi ve düşük çalışma sıcaklığı ile bir başka yakıt hücresine göre geliştirilmiş bir performansa sahiptir, proton değişimli membran yakıt hücresinin dinamik modeli MATLAB/Simulink

üzerinde geliştirilmiştir. Yakıt hücresi sisteminin modellenmesi için elektrik eşdeğer devreleri, yakıt hücresinin termodinamik özelliği ve iki katmanlı şarj etkisi kullanılır.

Bu model, geçici koşullar yanında geçici durumdaki PDM yakıt hücresi yığınının elektriksel tepkisini bekleyebilir. Ayrıca, bu model yakıt hücresi yığınının sıcaklık tepkisini tahmin edebilir ve Proton değişimli membranlı yakıt hücreleri için dış denetleyici tasarım uygulamalarında yararlı olabileceğini gösterebilir.

**Anahtar Sözcükler** : Dağıtık enerji kaynakları, mikro şebeke, proton değişimli membran yakıt hücresi, MATLAB/Simulink.

**Bilim Kodu** : 905.1.173

## **ACKNOWLEDGMENT**

I am highly grateful to the head and all teachers of the Electrical-Electronics Engineering Department, Karabuk University who took the time to offer me guidance. My deep gratitude goes to my advisor, Assoc. Prof. Dr. Ziyodulla YUSUPOV, for his close supervision, guidance and constant encouragements throughout an extended period of the study and the work.

I would like to thank my great mother, my lovely wife and children, friends for their encouragement, support, and unwavering love, which makes my dream come true.

## CONTENTS

	<u>Page</u>
APPROVAL.....	ii
ABSTRACT.....	iv
ÖZET.....	vi
ACKNOWLEDGMENT.....	viii
CONTENTS.....	ix
LIST OF FIGURES .....	xi
LIST OF TABLES .....	xiii
SYMBOLS AND ABBREVIATIONS.....	xiv
INDEX.....	xiv
CHAPTER 1 .....	1
INTRODUCTION .....	1
1.1. BACKGROUND .....	1
1.2. MOTIVATION OF THESIS.....	2
1.3. LITERATURE REVIEW.....	2
CHAPTER 2 .....	7
DISTRIBUTED ENERGY RESOURCES .....	7
2.1. BACKGROUND .....	7
2.2.SOLAR PHOTOVOLTAIC SYSTEMS.....	8
2.3. WIND ENERGY COVERSION SYSTEM.....	10
2.3.1. Wind Energy System.....	10
2.4. SMALL-SCALE HYDROELECTRIC POWER GENERATION .....	11
2.4.1. Power Plant Types And Their Technology .....	12
2.4.2. Environmental Influences.....	13
2.5. MICRO-COMBINED HEAT AND POWER SYSTEMS.....	13
CHAPTER 3 .....	16
FUEL CELL SYSTEM .....	16

	<u>Page</u>
3.1. OPERATION PRINCIPLE OF FUEL CELL .....	16
3.2. TYPES OF FUEL CELL.....	17
3.2.1. Alkaline Fuel Cells (AFC).....	17
3.2.2. Phosphoric Acid Fuel Cells (PAFC) .....	19
3.2.3. Molten Carbonate Fuel Cell (MFC) .....	20
3.2.4. Solid Oxide Fuel Cell (SOFC).....	21
3.2.5. Polymer Electrolyte (PEFC).....	22
3.3. FUEL CELL EQUIVALENT CIRCUIT .....	26
CHAPTER 4 .....	31
MATHEMATICAL MODELLING OF PEMFC .....	31
4.1. NOMENCLATURE PEMFC.....	31
4.2. PEM FC DYNAMIC MODEL DEVELOPMENT .....	33
4.3. GAS DIFFUSION IN THE ELECTRODES.....	35
4.4. PEMFC MODEL STRUCTURE .....	37
4.5. EQUIVALENT ELECTRICAL CIRCUIT MODEL OF PEMFC.....	38
CHAPTER 5 .....	45
MODELLING AND SIMULATION OF SR-12 PEM FUEL CELL ON SIMULINK /MATLAB.....	45
5.1. SPECIFICATION OF SR-12 PEMFC .....	45
5.2. MODELLING OF PEMFC BLOCKS .....	47
5.3. RESULTS OF SIMULATION.....	55
5.4. CONCLUSION AND FUTURE WORKS.....	61
REFERENCES.....	63
RESUME .....	66

## LIST OF FIGURES

	<u>Page</u>
Figure 2.1. Types of distributed generation .....	7
Figure 2.2. Stand-alone of solar photovoltaic system .....	10
Figure 2.3. Wind turbine with changeable speed pitch-regulated.....	11
Figure 2.4. Small hydroelectric power plant.....	13
Figure 2.5. Gas turbine or engine with heat recovery unit.....	15
Figure 3.1. Process of fuel cell .....	17
Figure 3.2. Fundantal of AFC .....	18
Figure 3.3. PAFC details.....	20
Figure 3.4. Block diagram of molten carbonate fuel cell.....	21
Figure 3.5. PEM FC anode and cathode Layers.....	22
Figure 3.6. PEM FC system anode-cathode reaction.....	23
Figure 3.7. The temperature of effect on fuel cell .....	28
Figure 3.8. Fuel cell loss division .....	29
Figure 3.9. Fuel cell Performance .....	30
Figure 4.1. Voltage drops of a PEMFC diagram .....	34
Figure 4.2. Block diagram of PEMFC .....	38
Figure 4.3. Block diagram of PEMFC to build electrical circuit.....	39
Figure 4.4. The equivalent circuit for internal potential $E$ .....	39
Figure 4.5. Activation loss electrical circuit model in PEM FC.....	41
Figure 4.6. Electrical circuit model of ohmic voltage drop in PEMFC .....	42
Figure 4.7. Concentration voltage drop circuit for PEMFC .....	43
Figure 4.8. Equivalent electric circuit of thermodynamic model for PEMFC.....	44
Figure 5.1. Model of SR-12 PEMFC on MATLAB/Simulink .....	47
Figure 5.2. The model active pressure of gas diffusion at electrodes on MATLAB/Simulink .....	48
Figure 5.3. The model of internal potential $E_{CELL}$ and $\Delta G$ on MATLAB/Simulink ..	49
Figure 5.4. The model of ohmic voltage drop on MATLAB/Simulink.....	49
Figure 5.5. The Model of concentration voltage drop on MATLAB/Simulink.....	50

	<u>Page</u>
Figure 5.6. The model of activation voltage drop 2 on MATLAB/Simulink .....	50
Figure 5.7. The model of activations voltage drop1 on MATLAB/Simulink.....	50
Figure 5.8. The model of drop delays block on MATLAB/Simulink.....	51
Figure5.9. Equivalent circuit of the double-layer charging effec inside within PEMFC .....	52
Figure 5.10.The model of terminal voltage on MATLAB/SIMULINK .....	53
Figure 5.11. The model Heat of Sensible + Latent on MATLAB/Simulink .....	54
Figure 5.12. Simulation result of PEM fuel cell current .....	56
Figure 5.13. Simulation result of PEM fuel cell voltage.....	56
Figure 5.14. Simulation result of PEM fuel cell iutput power .....	57
Figure 5.15. Simulation result of PEM fuel cell output temperature .....	57
Figure 5.16. Block diagram of PEMFC DC/DC converter – DC/AC inverter – load system .....	58
Figure 5.17. Simulation block of DC/DC converter onMATLAB/Simulink .....	58
Figure 5.18. Voltage of DC/DC converter on MATLAB/Simulink .....	58
Figure 5.19. Simulation block of DC/AC inverter on MATLAB/Simulink. ....	59
Figure 5.20. Current results of DC/AC inverter.....	59
Figure 5.21. Voltage results of DC/AC inverter .....	60
Figure 5.22. AC power results of DC/AC inverter .....	60
Figure 5.23. Simulink model of SR-12 PEMFC DC voltage in MATLAB/Simulink with converter and inverter to load.....	61

## LIST OF TABLES

	<b><u>Page</u></b>
Table 3.1. Effects of toxics on different types of fuel cells .....	24
Table 4.1. Analogies between electrical and thermodynamic parameters .....	44
Table 5.1. Electrical parameters of SR-12 PEMFC .....	46
Table 5.2. Specification of SR-12 PEMFC .....	47



## SYMBOLS AND ABBREVIATIONS INDEX

### ABBREVIATIONS

MG	: Microgrid
CHP	: Combined Heat and Power
DER	: Distributed Energy Resource
LV	: Low Voltage
PV	: Solar Photovoltaic
DG	: Distributed Generation
MT	: Microturbine
ICE	: Internal Combustion Engine
FC	: Fuel Oxide Fuel Cells Cell
SOFC	: Solid Fuel Cell
PEFC	: Polymer Electrolyte Fuel Cells
PEMFC	: Proton Exchange Membrane Fuel Cells
AFC	: Alkaline Fuel Cells
PAFC	: Phosphoric Acid Fuel Cells
MCFC	: Molten Carbonate Fuel Cells
H <sub>2</sub> O	: Water
H <sub>2</sub>	: Hydrogen
He	: Helium
O <sub>2</sub>	: Oxygen
CO <sub>2</sub>	: Carbon Dioxide
K <sub>2</sub> CO <sub>3</sub>	: Potassium Carbonate
Y <sub>2</sub> O <sub>2</sub>	: Yttrium Oxide
PEM	: Proton Exchange Membrane
MC	: Molten Carbonate
SO	: Solid
PA	: Phosphoric Acid.

## CHAPTER 1

### INTRODUCTION

#### 1.1. BACKGROUND

Last decades with rapidly integration of distributed energy resources to the power system, the interest on Microgrid (MG) is growing. MG is a basic element and a key component of Smart Grid. According to USA Department of Energy Smart Grid is the grid that integrates advanced sensing technologies, control methods, and integrated communications into the current electricity grid [1]. MG combines distributed energy resources, such as PV, wind, microturbines, fuel cells, combined heat and power (CHP), storage devices (flywheels, energy capacitors and batteries) and flexible loads, and connected to the power grid via switches. Generally, MG based on CHP simplify high efficient energy generated by holding waste heat. On other hand, the low carbon of distributed energy resources (DER) helps by generating clean power to decrease environmental pollution. Choices of DERs depend on the climates and topologies of the area and fuel availabilities.

A fuel cell typically refers to the hydrogen-oxygen fuel cell. A fuel cell is no energy storage, but it is a converter. The energy is supplied in chemically bonded form with the fuels.

The production of electrical energy from chemical energy is mostly done by incineration and recovery of the hot gases in a heat engine with a downstream generator. Thus, only is chemical energy by combustion in thermal energy and then into mechanical work converted. Only from this current is generated in the generator.

However, a fuel cell is suitable for achieving the transformation without the conversion into heat and power and is therefore potentially more efficient. Unlike an

internal combustion engine (ICE) directly, transfer the chemical energy to electrical energy without poor efficiency.

Theoretically, just by the free energy that limited the chemical reaction can achievable useful work, which may be more than in the coupling of a heat engine (Carnot efficiency) with a generator to produce electricity. Practically also with the combination of fuel cell and electric motor achieved efficiency higher than that of gasoline or diesel engines. However, in the entire chain of action, the expenditure for the production and storage of energy are considered with well researched, the hydrogen-oxygen fuel cell [2].

## **1.2. MOTIVATION OF THESIS**

In the last decades with development of information technologies and power electronics interfaces created a new concept “Smart Grid”. A basic element and a key component of Smart Grid is Microgrid. Microgrid consists of distributed energy resources such as wind and solar energy, micro-combined heat and power, fuel cells and group of loads that are considered in LV distribution network system.

In addition, the fuel cell is one of the type of distributed generation has intensive attention of researchers. The main problems in the power systems with providing security and efficiency of the system there is necessary to reduce greenhouses gases and carbon dioxide emissions. So, development of fuel cell model to consider operation, control and maintenance of fuel cell integrated to microgrid are of the first and basic thing.

## **1.3. LITERATURE REVIEW**

In fact, with advantages properties the hydrogen is a good energy transporter, nowadays, the fuel cells with hydrogen started be taken a good energy transporter, because they transform the chemical energy to electrical energy directly and effectively. In the 19th century, the fuel cells was invention as energy conversion system. While with stared of the 20th century the conversion of chemical energy into

electrical energy start be more and more important, because of raising request of electricity [1].

In the future, the energy needs has been classified as major problems that humanity must faced. The world now, the fossil fuels are primary energy that inclusive oil, coal and natural gas. But in fact that resources has some problems with the continued use of fossil fuels. The fossil fuels are limited quantity, which we know that one day it will finish. As well as limitation the fossil fuels rise serious environmental problems like global warming, air pollution, climate change, acid rain, and depletion of the ozone layer. The needs for alternative energy increasing day by day, which is combined with the fuel cell. The hydrogen energy system it may a good choice [2].

As electrochemical system, the fuel cell transforms chemical reactivity to electrical energy and that done by merge between the hydrogen and oxygen. The reaction output are hot and water. Fuel cells are higher efficient from traditional systems, where they have a lot of features that given advantages more than that in traditional systems of generate electricity. Spectacular feature, given to proton exchange membrane (PEM) of fuel cells, because of its advantages such as light weight, power, low cost [2].

As results of all those advantages, the researchers think fuel cells will be the most promising power generation equipment candidates for portable electronics, automotive and distributed power generation applications in future [3].

Sequential, the activities and application have been development of fuel cell by researchers. Although the proton exchange membrane technology has greatly improved, but unfortunately problems such as stability and reliability is not enough to take place from the internal combustion engine. As well as the high cost of fuel cell system that affect in it as commercial products. Moreover, important case to control is to improve its performance and reduce costs [4].

The hydrogen and air humidification in the PEM fuel cell sometimes needs to prevent dehydration of the fuel cell membrane because of high current flow, which is an ohmic heating that driven to slow ion transfer throughout the membrane as well as

drying problems in the polymer film. Since water is generated on the airside, no humidification is required in some fuel cell stacks. In a typical fuel cell system, hydrogen or air or both hydrogen and air at the fuel cell inlet are required to be humidified. significant ohmic losses, will happen if membrane dehydration or drying occurs, that give import ants to water content for proton conductivity in proton exchange membranes [5].

There is important to using the maximum power point tracking (MPPT) controller for practical applications due to the fuel cell non-linear property of P-I Junsheng et al. Proposed a Fuel cell and converting, using sliding mode control based on a mathematical model and a new approach to MPPT. In their method DC-DC converter to change the duty cycle of reinforcement Control is applied. The features of the controller are confirmed by simulations. The performance of the method of its good transient response, low tracking error and operational temperature, water content and load changes are very rapid system response. They proofed that their method can be applied effectively and economically [6].

Current and voltage that utilize non-linear and single maximum power point (MPP) can be used to generate fuel cell power. This path is an extreme MPPs by asking the paper controller to report the first attempt. Fuel cell MPP operating conditions of linear changes, there are no unforeseen changes. Therefore, the MPPT controller is required to change under operating conditions to ensure the highest power continuous load occurs. The intermediate converter is produced and designed with a dual loop cascade control unit to operate from the MPPs fuel cell powered system, the recommended combination of MPPT controls, fuel cells can continue to run, no real-time MPP provides a simple and powerful control law. Simulation of this control method, the fuel cell in the stability of the operating conditions change shows satisfactory results [7].

Fuel Cell and Power Optimization method of Maximum Power Point Tracking (MPPT) is one of technologies that is applied to improve power system efficiency and ratability. Perturb and Observations (P & O) Methods of Increasing Conductivity (IC) were simulated and compared favorably with FC system applications to determine which one [8].

Fuel cell (FC) low pollution, low noise, high efficiency. However, given a set of results, the response of the FC voltage-current to a single operating point of operating conditions maximizes the output power, which is non-linear. Therefore, the maximum power point tracking extension theory based on the existing research (MPPT) control scheme proposes a stable FC output at the maximum power point, hydrogen simulations confirm the ability of the controller to compensate for output power at the maximum power point despite abrupt changes in pressure up to membrane moisture content. In addition, the proposed transient response time of the controller, faster seeking sliding mode controller and termination has been shown to be present [9].

To maximize the efficiency of fuel cell power generation a new control strategy considered in [10]. The maximum power point tracking (MPPT) controller is based on the extreme value optimization control algorithm design. This closed loop can be done based on control methods of extreme perturbations, such as unacceptable by traditional optimization methods, such as the rapidly changing working conditions, obtained under the guarantee and observe the algorithm [10].

The ability of the system to generate energy as a fuel is limited. Therefore, MPP needs to be forced to work in exchange for maximum fuel cell power point system requirements. Fuel cell MPP is a unique constant point operation, load power requirements will change with the load resistance changes, the output voltage changes will not be taken into account. The CEO of Battery Fuel has put forward the necessary control measures, and proposed a new configuration and analysis for hybrid system. The fuel cell system runs its own MPP and works in a way that keeps the voltage constant. The proposed system operates under an acceptable range of work under different conditions [11].

Gain DC boost gain to make MFC a sensor less power-aware power management cell array (EA-PMU) with inductor less DC-DC (MPPT). Thanks to the MFC's power curve changes identified and selected at the optimal harvest point, increased efficiency and overall power distribution. At present, the problem of reverse voltage and current in MFC series or MFC applications is limited due to the parallel connection; this leaves a new maximum power point (MPP) every time. However,

each time you need to leave a new maximum power point (MPP). The converter maximizes efficiency and the available dynamic MPP adaptation adjusts power consumption. The converter is designed and fabricated in a 0.18 micron CMOS process with an input power of 1.6 mW and an efficiency of 65% [12].



## CHAPTER 2

### DISTRIBUTED ENERGY RESOURCES

#### 2.1.BACKGROUND

Last decades the power systems are facing problems such as gradual exhaustion of existing natural energy resources, pollution of the environment, which created the need for local power generation through fuels energy. Power production system of this type is called Distributed Generation (DG) and resources that used for this type generation is called distributed energy resources (DER). In Figure 2.1 is illustrated the types of DG.

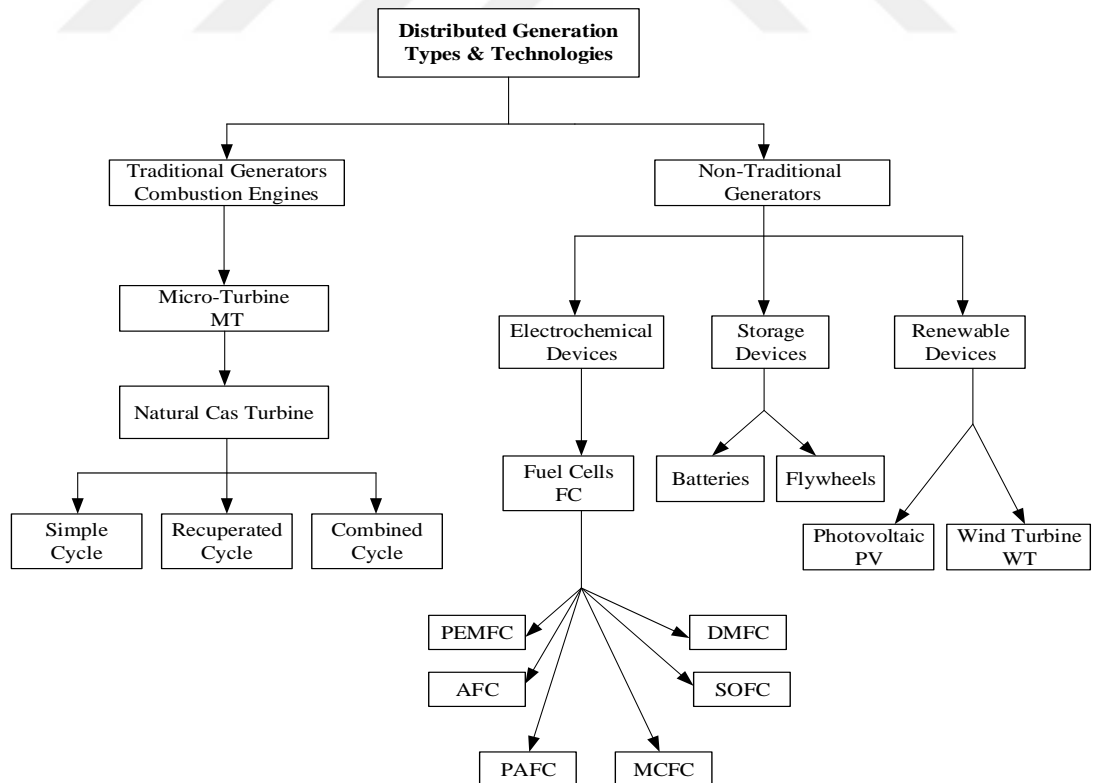


Figure 2.1. Types of distributed generation.

## 2.2.SOLAR PHOTOVOLTAIC SYSTEMS

A photovoltaic system, also known as a solar cell system, is a solar power system in which a part of the solar radiation is converted into electrical energy by means of solar cells. A larger solar power system is a solar power plant. The typical direct type of energy conversion is known as photovoltaic. On the other hand, other solar power plants (solar-thermal power plants) operate through the intermediate steps of heat energy and mechanical energy. The performance of conventional photovoltaic systems ranges from low single-digit kW ranges, as is customary for roof-mounted systems, to a few MW for commercial roof systems, while free-field solar systems are usually located in the MW range [13].

Depending on the system size and type, individual solar modules are connected in series to so-called strings. The solar modules, in the technical application, the smallest components of a solar system to be distinguished, consist of a series connection of solar cells which are hermetically encapsulated and are no longer accessible for repair. In the case of crystalline solar cells, the individual cells are initially produced individually and finally bonded by metal foils. In the case of thin-layer cells, the preparation of the compounds is integrated into the processes for forming the cells.

The voltage is then added by the series connection of initially solar cells, with a voltage of only about 0.5 V, and then solar modules. If the maximum system voltage was limited to 110 V 20 years ago, in order to meet the safety requirements, a system voltage of 1000 V is tested by today's solar modules according to protection class II, a further increase to 1500 V DC, the limit value of the low voltage definition according to VDE 100 is worked.

A square, crystalline solar cell with an edge length of 156 mm provides approximately 8 A in the operating point at maximum solar irradiation. The current through this series circuit is determined by the solar cell with the lowest current. In parallel, the currents of the individual strings are added. A parallel connection of individual modules is found in the isolated mode [13, 14].

The solar modules are generally mounted on a substructure, which ideally aligns the modules to ensure the highest possible or the same energy yield over the year (eg in Germany towards the south and angled at about 30 for the highest energy output and / Oriented towards the south and angled at about 55 for the most consistent energy yield over the year). The substructure can also follow the sun (astronomical, sensory) in order to achieve a higher energy yield.

In this situation of a grid-connected unit, the direct current generated in the solar module (s) is converted into alternating current and fed into the power grid. Apart from the conversion losses, this usually occurs completely as long as the network is available in sufficient quality (voltage / frequency). A demand-dependent feed-in (feed-in management) was binding in Germany with the new version of the feed-in law 2009 for plants over 100 kW [15].

Network-coupled photovoltaic systems do not provide the power grid with a normal power supply, since a maximum of regenerative energy is to be generated. However, systems with a peak power of 100 kW or more should have ability to minimize their power remotely by the network operator in the event of network overloads. Inverters can, if required, also supply or absorb reactive power into the grid, which is also required in the medium voltage directive since mid-2010, by means of more powerful systems which feed into the medium voltage level. Due to the now relevant performance of the photovoltaic plants installed in Germany (as at the beginning of 2013: about 32 gigawatts of peak power), photovoltaics is increasingly integrated into grid regulation. Therefore, a corresponding directive for the low-voltage grid in Germany was adopted in August 2011.

In the case of non-network systems, the energy is temporarily stored, unless it is used directly. Storing in energy storage, usually lead accumulators, requires the use of a charger. In order to be able to utilizing the stored energy for conventional electrical appliances, it is converted into alternating current by means of an island inverter.

For network-connected systems with storage systems, the trend towards lithium storage is now recognizable. Advantage: smaller dimensions with the same storage

capacity. Disadvantage: price more expensive in the Figure 2.2 is shown Stand-alone of solar photovoltaic system.

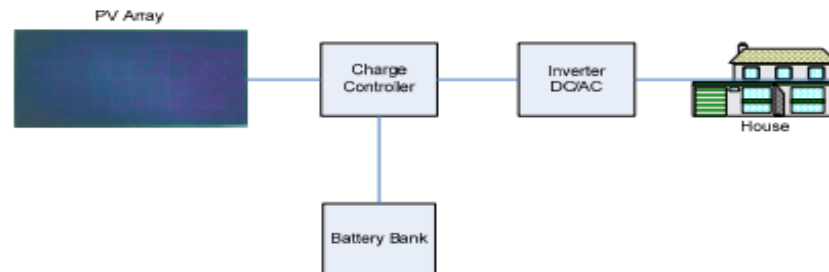


Figure 2.2. Stand-alone of solar photovoltaic unit [13].

## 2.3.WIND ENERGY CONVERSION SYSTEMS

Wind energy or wind power is a renewable energy source. The kinetic energy of wind, ie moving air masses of the atmosphere, is used technically. Wind energy has been used since antiquity to make available energy from the environment for technical purposes. While in the past it was mainly used with windmills or sailing boats, today's generation of wind power is by far the most important form of wind energy use. Other modern applications can be found in the mostly non-commercial sailing industry [16].

### 2.3.1. Wind Energy System

Wind energy is one of the most common renewable energy sources due to its worldwide availability, low cost and technological development. It now ranks among the mainstream technologies in electrical energy production and plays a central role in energy policy and energy strategies in a growing number of countries on the planet, due to technological advances and economic competitiveness in many markets around the world [17].

Wind energy plants can be used in all climatic zones, at sea and all land sites (coast, inland, mountains) to generate electricity. Therefore, a distinction is often made only between the use of wind energy on land (onshore) and the use at sea in offshore wind

parks. Up to now wind energy is particularly important on land, while offshore wind energy is still a niche market in the world, with 2.8% of the installed capacity. The dominance of the onshore sector is also expected in the long term, albeit with an increasing share of offshore installations. In the Figure 2.3 is shown wind turbine with changeable speed pitch regulated.

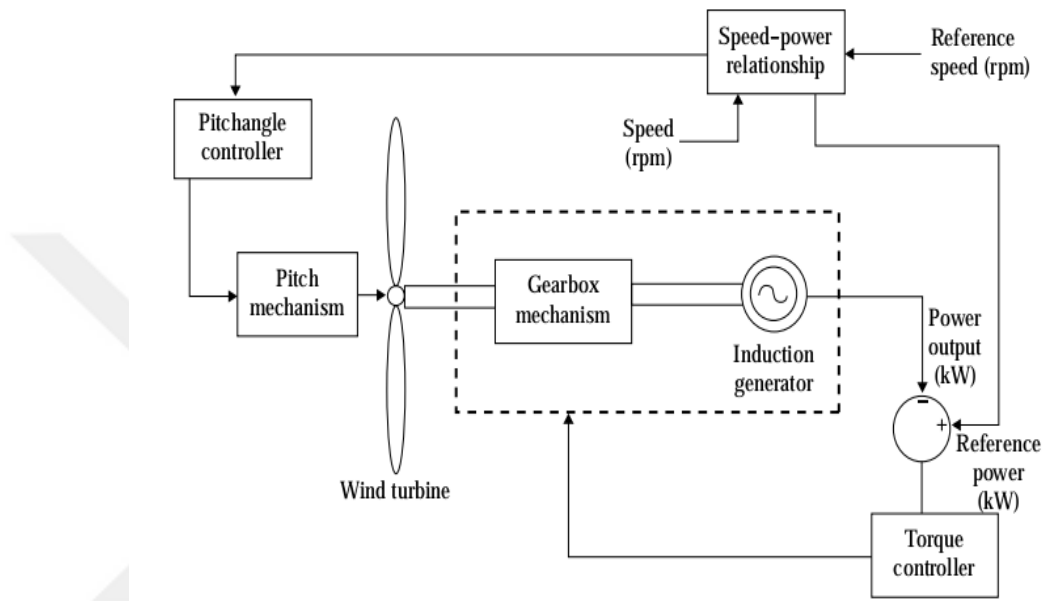


Figure 2.3. Wind turbine with changeable speed pitch regulated [17].

## 2.4.SMALL-SCALE HYDROELECTRIC POWER GENERATION

Small hydropower refers to the use of hydraulic energy by decentralized, small hydropower plants. In Germany, the limit is indicated at approx. 1 MVA, in Europe plants with a capacity of up to 10 MVA are designated as small water power plants, this limit is arbitrary and in some countries it is higher, eg China 30 MVA. Small hydropower plants operate on the same principle as large hydropower plants. They differ primarily in the performance class. There are, however, technical and historical differences [18].

Small hydro power plants are available in very different versions. Most of the facilities are located on small rivers and do not have a storage lake, but over water basins of different size and type. Plants with storage capacities can contribute to decentralized energy storage. Doping plants feed the water with residual water below

large Reservoirs Island systems do not feed into the grid, but supply consumers in remote areas. Such systems are widespread in many developing countries. Classical hydroelectric power plants use the potential energy in rivers and are therefore run-of-the-river power stations. Drinking water plants use the excess pressure in water supplies, which are fed from springs in elevated positions. The majority of hydroelectric power plants belong to the category of small hydropower; the proportion varies widely depending on the region. The history of small hydropower in Western Europe is closely linked to the history of industrialization. In the middle Ages, waterwheels were used to power mills and machines at tens of thousands of locations. Gradually in the 19th century the competition grew by the steam engine, which could be used more independently from local conditions. At the same time, the technology of small-scale hydropower plants continued to develop. For example, mill wheels were replaced by Francis turbines at the beginning of the 20th century, and increasingly the plants of electricity production instead of the mechanical energy generation (also referred to as "current mills") were used. The development was very different from region to region. In Switzerland, for example, the Eastern Mittelland or the canton of Glarus belong to the regions with a high density of traditional small-scale hydroelectric power [19].

#### **2.4.1. Power Plant Types And Their Technology**

The smallest form of a small hydroelectric power plant is currently the hydroelectric power plant. This type draws water into a flowing water with the aid of a short concrete ramp and feeds it to a circular concrete basin with drainage. The resulting water vortex drives a specially shaped vortex rotor, which generates current through the resulting torsional force. Turbines transform the energy of the water from a height of 2 m. Tube and capillary turbines are suitable for this purpose. Francis and particularly the more elaborate Pelton turbine is used for larger falls. In addition to synchronous generators, asynchronous generators are also used as generators.

However, the latter cannot provide a reactive power in the network, which is required for regulation and stabilization in alternating current networks. For this reason, asynchronous generators are only used in smaller plants [20].

### 2.4.2. Environmental Influences

Like every form of energy use, small water power has an impact on the environment, proponents of small-scale hydropower argue that the waters did not pollute the waters, or at least less than large power plants, according to the latest standards and suitably constructed small-scale hydroelectric power stations. Fish rises and ecological accompanying measures, such as those financed through green electricity labeling, could avoid damage and often lead to an improvement. Opponents of small water power argue that small plants are no better than large ones. Structures and insufficient amounts of residual water damage the ecosystems [18]. In the Figure 2.4 is shown Small Hydroelectric power plant.

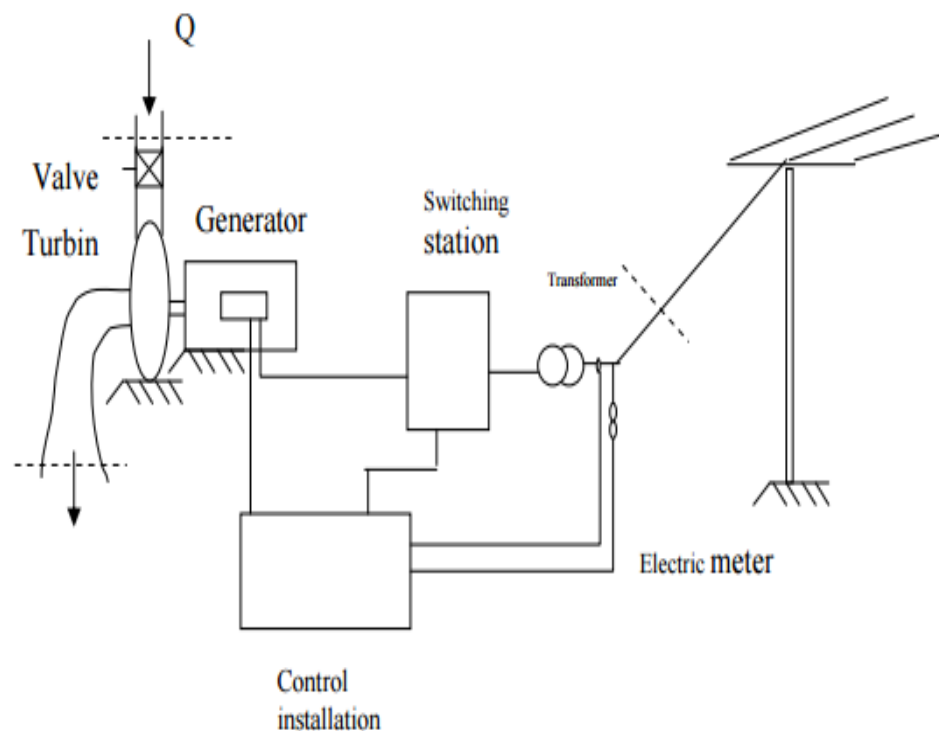


Figure 2.4. Small hydroelectric power plant [18].

### 2.5.MICRO-COMBINED HEAT AND POWER SYSTEMS

Micro-cogeneration (micro-cogeneration) covers the lowest power segment of combined heat and power (CHP) cogeneration plants. It is particularly suitable for building integrated use in houses as well as in the small trade [21].

The micro-cogeneration takes place mainly in the heating cell thanks to micro-cogeneration plants (micro-CHP) with waste heat utilization for domestic hot water heating and room heating. By decentralized energy conversion, it reduces electrical and, above all, thermal transmission losses and is characterized by a high exergetic degree of quality compared to pure combustion processes.

A second possibility is the differentiation according to the amount of annual electricity input, since as a rule no power measurement is carried out for small plants, on the consumer side, grid operators have to apply standardized load profiles. An electro technical standard for micro generators, is limited to a nominal value of up to 16 A per phase, three-phase around 11 kVA apparent power, which results in a power factor  $\cos \varphi = 0.9$  about 10 kW real power.

Furthermore, the cogeneration directive limits the term "cogeneration unit" to an output of less than 50 kW. There is also a further stage in the CHP Act for plants below 50 kW in the cogeneration surcharge on the generated electricity from cogeneration. The first "Impulse Program for Mini-CHP Plants" (September 2008) from the Federal Ministry of the Environment also had the 50 kW as the upper limit for the granting of an investment subsidy. Therefore, it is a good idea to name this somewhat broader class up to 50 kW mini-CHP [21].

The difference between micro-cogeneration and mini-cogeneration is that the former is mainly installed in an object-integrated manner, but the latter can also be supplied with small local heating networks. Both have in common the fact that they have the potential, as opposed to large cogeneration plants and combined heat and power plants, to enter mass production as a mass-produced product.

The subclass of electricity-generating heaters for single and double family houses is called Nano-CHP (or Nano-CHP). The electrical power is usually 1 kW, but other plant sizes are also available. A single-phase nominal current of up to 16 A is recommended as a demarcation, analogous to EN 50438 (requirement for micro generators), an apparent power of 3.68 kV. The units are supplied in combination with an integrated or external peak load burner (20-30 kW), which provides the

maximum heat load in winter [22]. In the Figure 2.5 shown gas turbine with heat recovery system [21].

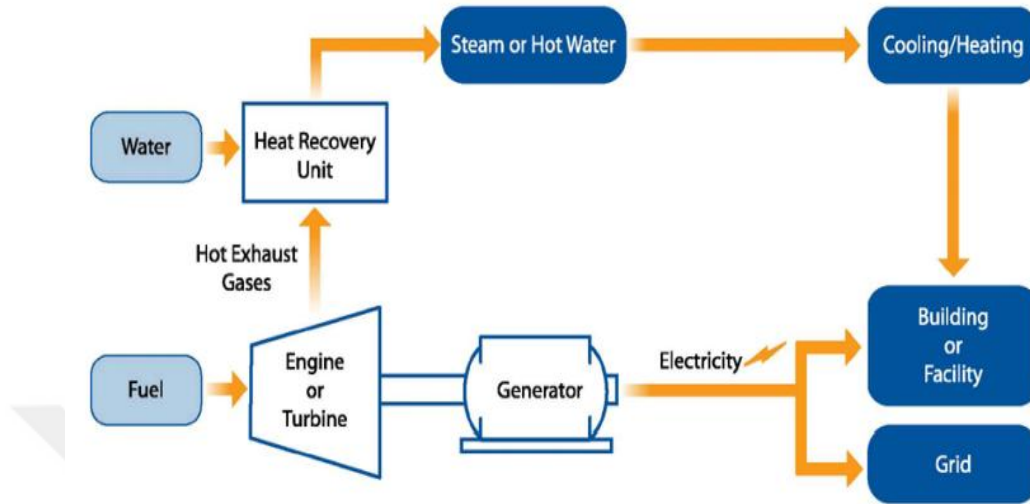


Figure 2.5. Gas Turbine with heat recovery unit [21].

## CHAPTER 3

### FUEL CELL SYSTEM

#### 3.1.OPERATION PRINCIPLE OF FUEL CELL

In Britain 1839, Sir William Grove, discovered bases of fuel cell, where the oxidation and reduction reactions were the idea to production the electric power, however, by the reason of high materials costs were very expensive fuel cell had used only in the space projects. In automobile industry fuel cell has been utilizing since mid of 1960's [23, 24].

Fuel cell is device that convert chemical energy to electrical energy without combustion. The hydrogen compounds like hydrocarbons and ammonia are used as a fuel for fuel cells. Fuel cells operate at high temperature, the shape of the voltage and current density graph changes [25, 26].

Cathode, anode and electrolyte are the major components of fuel cells. Generally, separation should be done to the hydrogen ions and free electrons after integration hydrogen molecules in the anode. Through the cathode, the hydrogen ions pass to face the oxygen molecules. Then started from the anode until facing cathode free electrons are moving and that moving done by different path called electrical current, moreover, the chemical reaction will finish at the cathode. All of the hydrogen atoms, oxygen molecules and free electrons produced processes of fuel cell shown in Figure 3.1 [27].

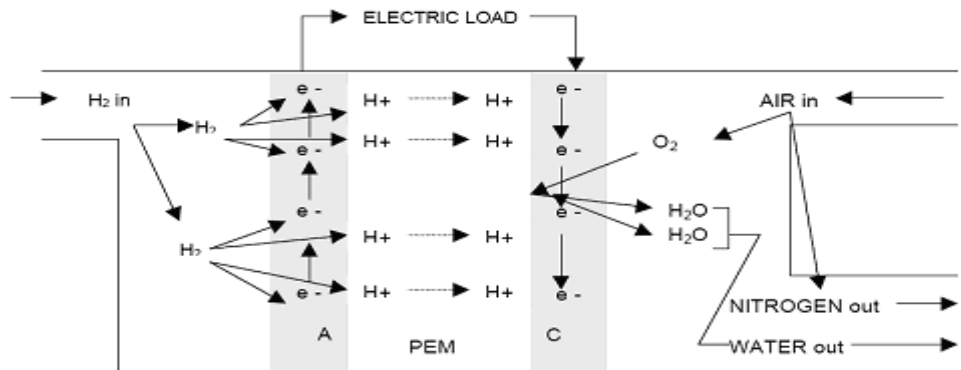
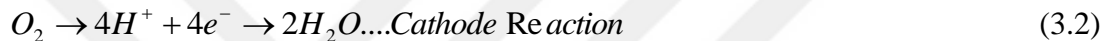


Figure 3.1. Process of fuel cell [27].



### 3.2. FUEL CELL TYPES

There are several types of fuel cells:

- Alkaline fuel cells (AFC).
- Phosphoric acid fuel cells (PAFC).
- Molten carbonate fuel cells (MCFC).
- Solid oxide fuel cells (SOFC).
- Polymer electrolyte fuel cells (PEFC).

#### 3.2.1. Alkaline Fuel Cells (AFC)

In addition, with 85% and 40% percentages those are the main two types of potassium hydroxide (KOH) electrolyte concentration, while the first operating temperature is 250 °C, which the lower and higher one is less than 1200 °C. This operation process used and development of AFC at 1960 that was the famous research named as Apollo Space Vehicle. Where, just the hydrogen is applicable as a

fuel supply, that because for example is hurtful as it tends to react with KOH to create at that time (AFC) was utilized to produced electric power for Apollo.

Regardless of its successfully, Alkaline fuel cells faced some difficulties such as sensitivity. Alkaline fuel cells AFC have some important features like many types of electro-catalysts are usable and so active electro kinetic, which make the Alkaline fuel cell's performance wonderfully. From other side, the Alkaline fuel cells needs high ratio of purity, which is means that CO and purification unit should be well-designed at high efficiency. Inclusively, the cost is getting high more and more, also the construction are disadvantage by getting more complex and the size is getting bigger [28, 29]. Essential reactions and common fuel reaction as following:



KOH is choosing as electrolyte because it is the best of alkaline hydroxides when match with conductance Figure 3.2.

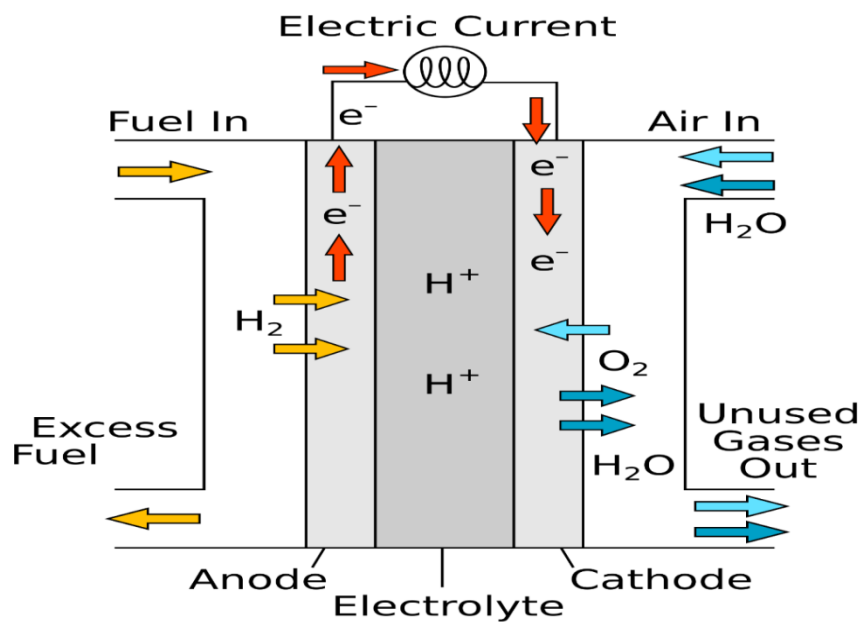


Figure 3.2. Fundamental of AFC [28].

### 3.2.2. Phosphoric Acid Fuel Cells (PAFC)

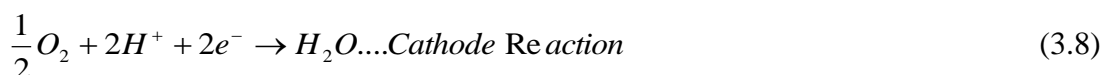
Generally, the fundamentals of PAFC concentration is started with 100% phosphoric acid and operating temperatures in between 150 °C and 220 °C, that high temperature raising the conductance with stopping CO to harm Pt catalyst [27].

Materials selecting for any trade product includes an iterative design process that eventually becomes specific to the special product and application [28, 29]. In addition, as results of high relative durability as well as consequence pressure of water vapor reducing that drive to water treatment simple, which advantage of low operation temperature of concentrated phosphoric acid, when you compared to common margins of acids. The Pt is utilizing in anode and cathode as well, moreover, as application of silicon carbide is used to keep acid healthy.

In fact, the PAFC was designing and present to be compatible to those systems that make PAFCs feasible as settled systems. Nowadays, PAFC simple system and possible to find PAFC and it modern system in USA or Japan. But recent developments on PEFC reducing popularity of PAFCs because of better performance and lower cost [28, 30].

Overall, its components are viable for framework because of the operating temperature is lower. Therefore, CO sensitivity of PEFCs and AFCs are higher than PAFCs. That simplifies design and build up of systems to export heat from fuel cell, totally, system capacity is better than PEFCs, But on other side its worse than SOFCs and MCFCs. Platinum catalyst is highly needs and reduction reactions is lower than the AFCs. To upgrade the system performance, the sophisticated fuel operation system is major requirement. Since corrosion tendency of phosphoric acid is high, stack tools should be complex as a result stack cost becomes higher as well

In Figure 3.3 is shown PAFC details [27].



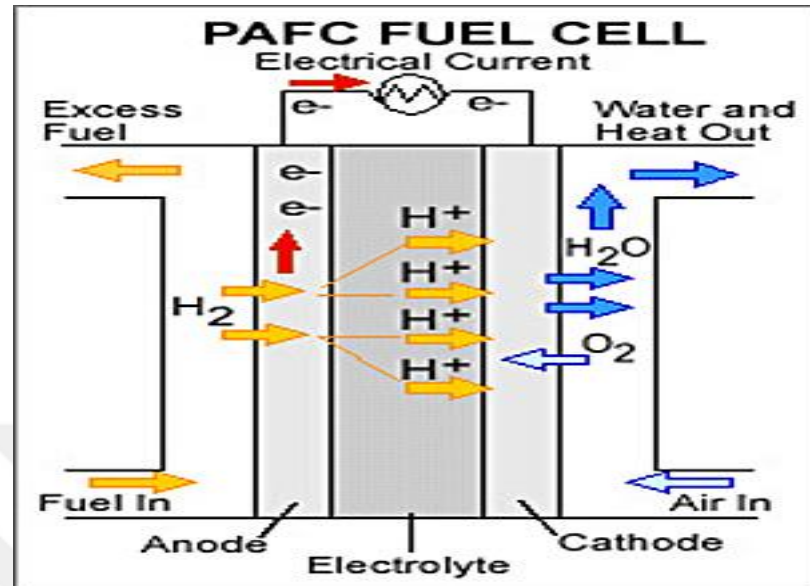


Figure 3.3. PAFC details [28].

### 3.2.3. Molten Carbonate Fuel Cells (MCFC)

Because electrolyte is content of alkali carbonates, which sitting up perfect electric conductive environment by carbonate ions in operation temperature between 600 °C and 700 °C. With these high temperatures, the enables to utilizing Nickel as anode where the cathode can be Nickel oxide. That given advantages such as low cost because of no need to noble metals to raising chemical activation [28, 30].

The major interest area of molten carbonate fuel cells is Marin industry that because of huge volumes and long starting time, which can be tolerated. In addition, because of High working temperature that may reach 650 °C – 700 °C. There is no need to high cost of electro catalysts. The Molten carbonate fuel cells systems are able to utilize CO or hydrocarbons as a fuel this raises system capacity up to middle fifties, as well as MCFC ability the CO management is not necessary because the construction will be simple. But, automotive industry applications the high temperature should be outsourced for this reason some additional cost, weight and volume [28, 30].

In some cases, two electrodes contacted with ceramic filled with the molten carbonate salt, which as electrolyte. Block diagram of molten carbonate fuel cells shown in Figure 3.4. On other side, some other disadvantage like high cost as result to utilize high-quality stainless steel because of electrolyte which tends to corrode other equipment [31].

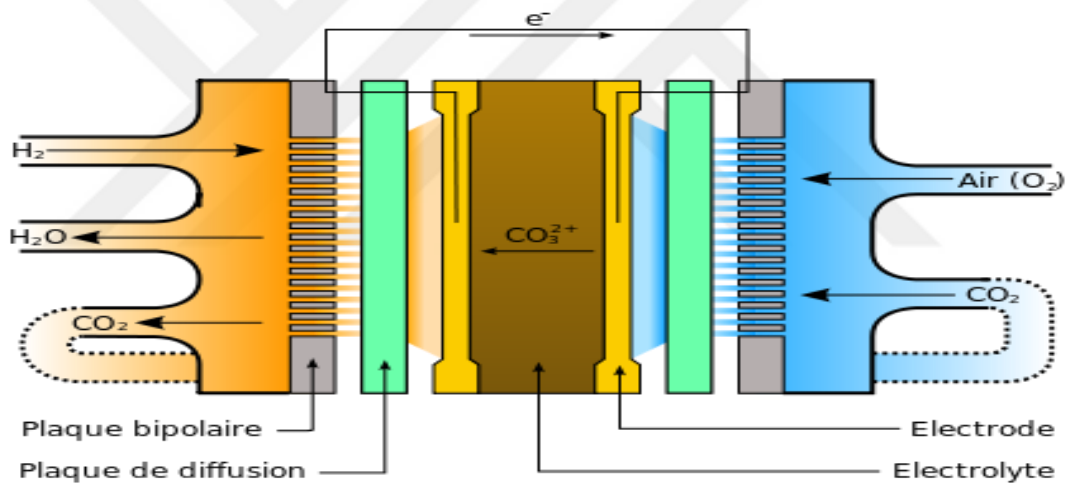
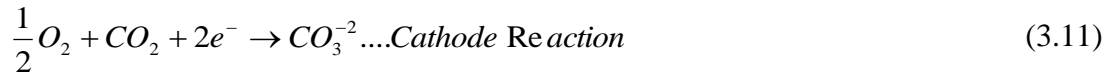


Figure 3.4. Block diagram of molten carbonate fuel cells [28].

### 3.2.4. Solid Oxide Fuel Cells (SOFC)

Normally, as solid electrolyte of SOFC are produced from Yttrium Oxide (  $Y_2O_3$  ) material. While the electrolyte takes some advantages like done without, corrosion and it can be management, all of that because, it's not a liquid also CO can be utilize as fuel. Generally, we can say it has a good capacity, performances and suitable for fast working conditions, but nominal in operation process the temperature is going to be high nearly 1000 °C which a problem and need to additional equipment to solve as a consequence the cost raising, the size gets bigger. In this case, if temperature

problems get solved SOFC can be utilizing in mobile applications as well. However, the applied load of SOFC should be slightly biting constant, because excessive load changes damage the unity of stack [27].

### 3.2.5. Polymer Electrolyte Fuel Cells (PEFC)

PEFCs get place as one of appropriate option for new hydrogen that based energy conversion systems, because of its advantages such as low operation temperatures and short response time as well as higher voltage current capacities. In the future, the hydrogen that producing from water and other renewable energy can fuel huge fleet of proton-exchange-fuel-cell vehicles [32].

Proton Exchange Membrane Fuel Cell (PEMFC), it the other name of PEFC, which content three mother parts. The ion exchange membranes the first part is that separates  $H^+$  and  $e^-$  is the conductive path. Porous layer is the secondly part, which works as a gas diffuser also as mechanical support, pathway for electrons and path for exhaust water from the electrodes, while the third part is contact electrodes between layer and membrane. PEMFC anode and cathode layers is showing in Figure 3.5 [30].

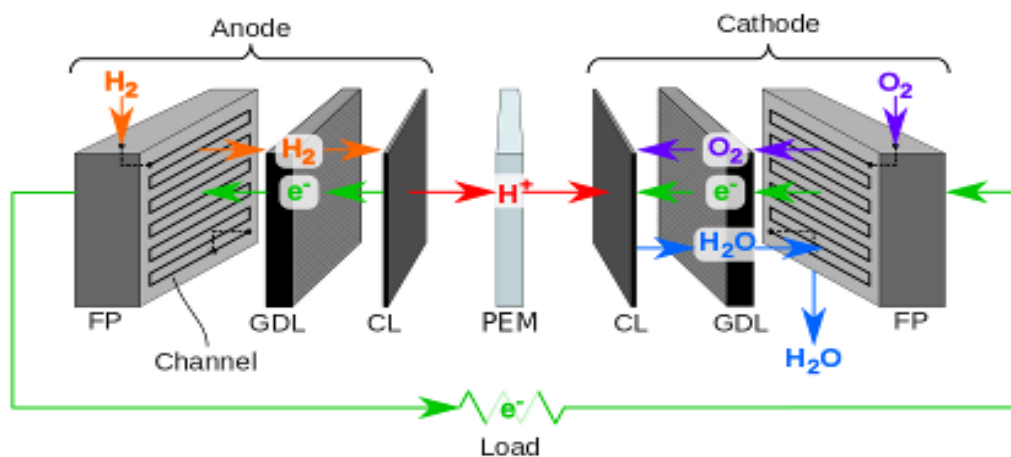


Figure 3.5. PEMFC anode and cathode layers [30].

The distribution of hydrogen and oxygen at the system are hydrogen oxidized  $H^+$  and  $e^-$  at anode while the hydrogen oxidation potential and at cathode side. Where,

oxygen reduction potential creates 1 V, which pulls H<sup>+</sup> ions from anode to cathode, PEMFC system (Anode-Cathode) reaction shown in Figure 3.6.

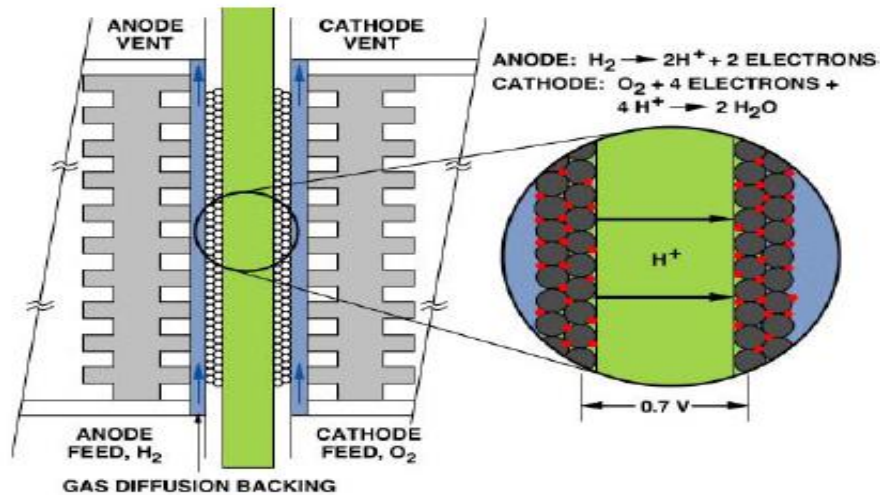


Figure 3.6. PEMFC system (anode-cathode) reaction [30].

In the last years, polymer electrolyte fuel cells PEMFCs, get a lot of attention as one of promising candidate for high efficiency, low-emission power resources [33].

Normal theoretic operation temperature of PEMFC is nearly between 0 – 90 °C, but in exponential operation a PEMFC works about 60 – 80 °C. In fact, PEMFCs system able to start up time fast from normal conditions that as results of low working temperature. However, low operation temperature lead to CO poisoning in some cases, because CO is felled for platinum catalyst at lower temperatures. The condition work at high temperatures more than 120 °C just enough to stop CO poisoning while in some work condition like low quantities of CO such as 2-3 ppm is pliable at 60 – 80 °C. Ideally, system membrane is producing from nafion (per fluorinated sulfonic acid polymer) and in some cases may cannot working properly at those operating temperatures since it dehydrates unless high pressure supplied [34, 35]. The output water will be liquid, if operating work pressure are equal ambient pressure as well as the operating temperature is below 100°C. That give important to water concentration for electrolyte ability conduction. The key issue for PEMFC are water treatment, which depends on work conditions, membrane and electrode properties. In addition, the critical topic is keeping work temperatures stable during

work that can be achieved by cooling water to hold temperature difference below 10 °C.

The high effective contaminants CO and S, CO<sub>2</sub> while hydrocarbon fuels comparatively low effective on PEMFCs. Sulfur content the most affected and in some cases damaging to the fuel cell, because sulfur components adsorb to the Pt catalyst and decreasing the number of available reactivity site for the oxygen reduction reaction. Some harmful chemicals components such as ammonia causes membrane deterioration, alkali metals and hydrocarbons harm catalyst. To prevent damage and performance loss of the fuel cell the air intake should be filtering as same as the internal combustion engine, dust should be removed in the intake system, in fact fuel cell content a lot of components that are sensitive to this impurity. In addition, some other harmful chemical substances should be removing as well. Fuel cells, several types and the effect of toxics in Table 3.1 [34].

Table 3.1. Several types of fuel cells and the effect of toxics.

Gas	PEMFC	AFC	PAFC	MCFC	SOFC
CO	Poison	Poison	Poison	Fuel	Fuel
CH <sub>4</sub>	Diluent	Poison	Diluent	Diluent	Fuel
CO <sub>2</sub> & H <sub>2</sub> O	Diluent	Poison	Diluent	Diluent	Diluent
S(H <sub>2</sub> S)	Diluent	Poison	Poison	Poison	Poison

PEMFC has two inputs in operation system, which are hydrogen and oxygen. Where the hydrogen is supplied from hydrogen storage unit while oxygen is taken from surrounding atmosphere by an air unit, which is used to get high performance and efficiency from a PEMFC. As same as pressure, humidity, flow-rate, temperature and purity, the input air has emphasis on performance of the PEMFC [35].

Fuel cell has two inputs one of them is Oxygen, as result of that the physical properties of oxygen highly affect in performance of the fuel cell. Probable also the oxygen pressure has positive effect in fuel cell performance.

As provable at operating temperature 93 °C performance fuel cell raising to 42 mV and when oxygen pressure changed from 3bar to 10 bar is 215 mA/cm<sup>2</sup>. In other reaction, at operation temperature 50 °C the oxygen pressure is raising from 1 bar to 5 bar, 500 mA/cm<sup>2</sup> and 83 mV are obtained. As same as previous example, current density of a PEMFC are raised to 431 mA/cm<sup>2</sup>, and voltage increase up 22 mV by only 1 bar pressure at temperature 80 °C. The effect of oxygen pressure has been proved, where with increased oxygen pressure improves the performance of PEMFC, however, compressing of oxygen is still work and still consumed amount of power, for that reason, there are needs for good optimization and the additional work to compress oxygen should be more than extra work that retched at fuel cell side [28].

Ideally, PEMFC current density is 200 mA/cm<sup>2</sup>, which gained 0.78 V at operating temperature 80 °C. As previous mention, the higher operation temperatures progress fuel cell performance such as 1,1-2,5 mV per each degree. Where the reason is highest operation temperature reducing ohmic resistance of electrolyte and raising reaction kinetics. Likely, operating temperature have positive effect on performance of fuel cell, however too much operation temperature increasing lead to dehydrogenation and it may decelerate ionic conductivity. The thermal management system should be removed extra heat, which normally air/water is preferred to keep PEMFC in optimum operation temperature. In fact pure oxygen performance is preferable than normal air, when utilizing the same air the high temperature lead to higher performance [28].

Utilize of H<sub>2</sub> for PEMFC direct need R&D especially work on heat exchangers, humidifier and condenser. Automobile industry standards limit engine highest operation temperature 60 °C [28].

Serious problem could be faced, which needs advanced water and heat treatment unit mostly in quite hot areas, because the operating temperatures different will be so small. Although, CO sensibility and thermal properties, PEMFCs looks like the higher suitable fuel cell system. For mobile applications, as well because low operation temperature and it can be ease build up with instantaneous changes in automobile applications by fast start up and good response abilities [34].

Likewise, working temperature of PEMFCs there is the best current and voltage capacities as well. However, some problems could be faced and they wait for to be solved. To solve that problem some procedures must be follow like reducing the volume and weight. Also, improve life and reliability features. Moreover, should be robust to run in different working conditions. Because people travel by their cars from a hot places to cold or sea areas at 1000 meters. Finally, the fuel cell cost and related systems should be coming down to be competitive of gasoline engine systems. The related systems of fuel is hydrogen, majorly storage systems and technical foundation should be built up and distributed, standards must be published as well [34].

Although it's the important just 100 hydrogen-refueling stations installed in all the World until now. The researcher expected raising in stations number in next short time. As overall evaluation, the fuel cell systems still higher cost than traditional combustion engine and cooling mechanisms also raise fuel cell stack cost, but in fact those problems are not only PEMFC's problems at the moment. We can classify those problems as general problems of new developed technologies. In fact, several attempts and offers have been made to model Proton Exchange Membrane Fuel Cell Stack (PEMFCS). Most of researches that endeavors was modeling [35].

### **3.3.FUEL CELL EQUIVALENT CIRCUIT**

Nowadays, PEM fuel cells considered as energy resources to provide reliable power at steady state, however they cannot respond to electrical load transients as fast as desired [37, 38]. Under fixed pressure, temperature conditions, the work condition are optimum with change in Gibbs free energy:

$$W_{el} = \Delta G = -n.F.E \quad (3.13)$$

n – number of electron in reaction;

F – Faraday constant;

E –optimum potential of the cell.

The Gibbs Free Energy Constant formula equals:

$$\Delta G = \Delta H - T.\Delta S \quad (3.14)$$

$\Delta H$  –enthalpy change

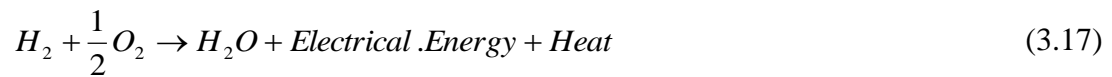
$\Delta s$  –entropy change

The negative entropy means the reaction generated heat, while positive entropy means the reaction needs heat. Fuel cell efficiency are:

$$\eta = \frac{\text{Beneficial Energy}}{\Delta H} \quad (3.15)$$

$$\eta_{ideal} = \frac{\Delta G}{\Delta H} \quad (3.16)$$

Basic reaction:



At normal conditions, 25°C and 1 atm.

$\Delta H$  285,8 H kJ/mole.

$\Delta G$  237,1 G kJ/mole.

The ideal efficiency can be calculated as:

$$\eta_{ideal} = 0.83 \quad (3.18)$$

$$\eta = \frac{\text{Beneficial Energy}}{\Delta H} = \frac{\text{Beneficial Energy}}{\left(\frac{\Delta G}{0.83}\right)} = \frac{V_{real} \times I_{real}}{\left(\frac{V_{ideal} \times I_{real}}{0.83}\right)} = \frac{0.83 \times V_{real}}{E_{ideal}} \quad (3.19)$$

In special work conditions where the hydrogen and oxygen, be pure 100% and work temperature and pressure are 25 °C and 1 atm the ideal potential  $E$  equals can be gained as also for liquid and gas (1.229 V and 1.18) of output water. At this case the equation is:

$$\eta = 0.675 \times V_{real(cell)} \quad (3.20)$$

While different work condition of water lead to changes in Gibbs free energy during the vaporization, which resulted a difference between ideal potential. as same as water , the temperature effect on ideal potential as well , next graphic given more details [28]. The temperature effect on fuel cell is showing in Figure 3.7.

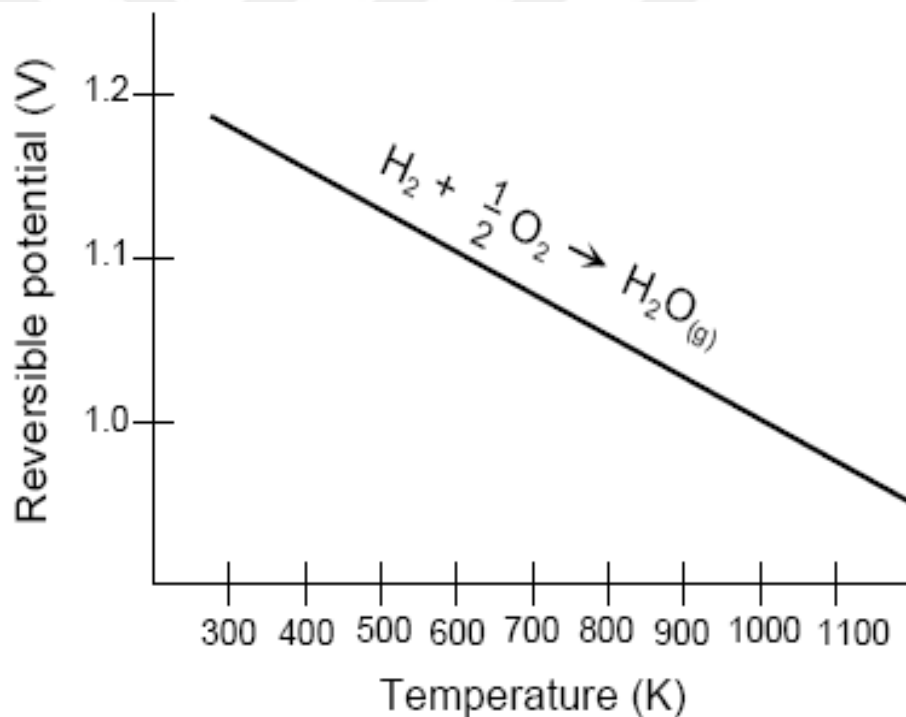


Figure 3.7. The temperature effect on fuel cell [28].

In fact, some reaction losses like reaction rate losses, ohmic losses because of electrolyte resistance to ion flow as well as gas transport losses and electrode resistance to electron, all of these non-reversible reasons lead to different between ideal and real. Fuel cell loss division in Figure 3.8.

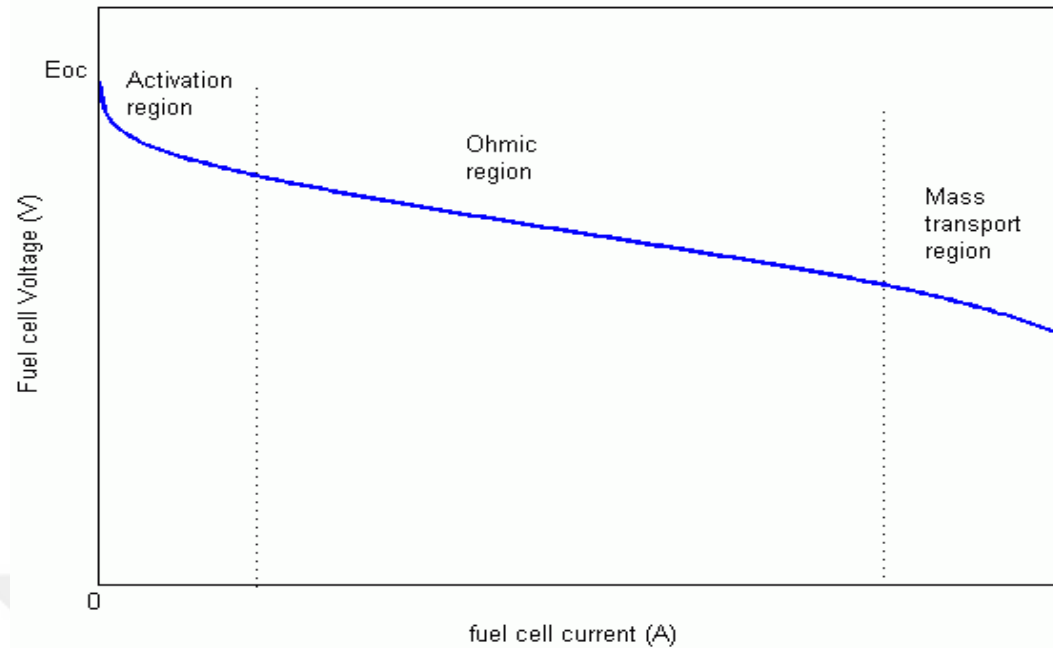


Figure 3.8. Fuel cell loss division [28].

In addition, the current comes as an important coefficient, especially the current density that seriously affected in performance of fuel cell. As reaction started, the current flows unless that reaction speed still low and voltage reducing, while through the normal operating, electrode and electrolyte start resistances that lead to voltage drop. Necessary reactant cannot pass cathode during high current ratio, because of voltage reducing. The relationship between voltage-current and power-current are showing in next figure. Where the minimum power means maximum voltage as well as lower current density. Moreover, optimizing should be handling in case of maximum power means minimum voltage and minimum cell efficiency. Fuel Cell performance showing in Figure 3.9.

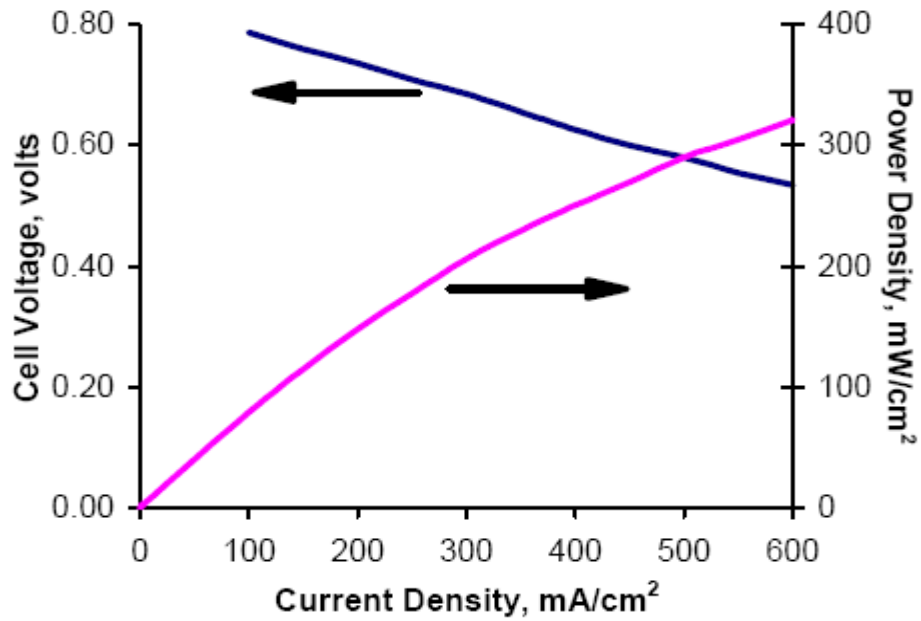


Figure 3.9. Fuel cell performance [28].

As same as current density, the temperature come as critical coefficient, which effect the cell performance with pressure. In addition, H<sub>2</sub> and C<sub>2</sub> reaction is exothermic and any raising in reaction temperatures will reducing potential (0.84mV/ °C) of the fuel cell. To improving cell, performance and increasing potential voltage the pressure should be positive changes. Unless pressure, the temperature have different effects in reaction, where with increasing temperature enhances electrode reactions, furthermore, on the contrary to normal conductive materials, any raising in reaction temperature, declines Ohmic resistance and promotes reaction.

## CHAPTER 4

### MATHEMATICAL MODELLING OF PEMFC

#### 4.1. NOMENCLATURE OF PEMFC

Most of the symbols and abbreviations used in the development of PEMFC model are defined and given below [33].

##### NOMENCLATURE PEMFC

$A, b$	Constant terms in Tafel equation (in Volts per Kelvin).
$A_{CELL}$	Area of each cell $m^2$
$E$	Reversible potential of each cell (in Volts).
$E_0$	Reference potential (in Volts).
$E_0^0$	Standard reference potential (in Volts).
$F$	Faraday constant ( 96487 Coulombs per Mol).
$h_{CELL}$	Convective heat transfer coefficient $W/(m^2) * K$ .
$H_v$	Vaporization heat of water (in Joules per Mol).
$I, i$	Current (in Amperes).
$I_{den}$	Current density $A/m^2$ .
$I_{limit}$	Limitation current (A).
$I_0$	Exchange current (A).
$K_E$	Empirical constant in calculating $E_0$ (in Volts per Kelvin).
$K_R$	Empirical constant in calculating $R_{OHMIC} [\Omega / A]$ .
$K_{RT}$	Empirical constant in calculating $R_{OHMIC} [\Omega / K]$ .
$I_a$	Width between anode channels to catalyst (in Meters).

$M_i$	Mole flow rate of species (in Mol per Second).
$N_i$	Superficial gas flux of species $i$ [ $mol/(m^2 * s)$ ].
$N_{CELL}$	Number of cells in the stack.
$P$	Pressure (in Pascals).
$P_i$	Pressure of compartment $i$ (in Pascals).
$p_i$	Partial pressure of species $i$ (in Pascals).
$q_{chem}$	Chemical, or heat energy (in Joules).
$q_{elec}$	Electrical energy (in Joules).
$q_{loss}$	Heat loss (in Joules).
$q_{net}$	Net heat energy (in Joules).
$q_{sens+latent}$	Sensible and latent heat (in Joules).
$R$	Gas constant, $8.3143 J/(mol.K)$ .
$T$	Temperature (in Kelvin).
$T_{ROOM}$	Room temperature (in Kelvin).
$T_{initial}$	FC initial temperature (in Kelvin).
$V$	Volume $m^3$ .
$V$	Terminal voltage (in Volts).
$V_i$	Voltage drop of type $i$ (in Volts).
$\chi_i$	Mole fractions of species $i$ .
$\chi$	Axis $\chi$ .
$z$	Number of electrons participating.
$\eta_0$	Temperature invariant part of $V_{act}$ (in Volts).
$\alpha$	Electron transfer coefficient.
$\Delta G_0$	Gibbs free energy at standard condition (in Joules per Mole).
$\lambda_e$	Constant factor in calculating $E_d(\Omega)$ .
$T_a$	Fuel flow delay (in Seconds).
$T_C$	Oxidant flow delay (in Seconds).
$T_e$	Overall flow delay (in Seconds).

### Superscripts and subscripts

A	Anode
Act	Activation
C	Cathode
Cell	Conditions For A Single Cell
Channel	Conditions At The Anode or Cathode Channel
CO <sub>2</sub>	Carbon Dioxide
Conc	Concentration
Consumed	Material Consumed In Chemical Reaction
Generated	Material Generated In Chemical Reaction
H <sub>2</sub>	Hydrogen
H <sub>2</sub> O	Water
In	Input
l(g)	Liquid (Gas)
N <sub>2</sub>	Nitrogen
O <sub>2</sub>	Oxygen
Ohm	Ohmic
Out	Output
Sat	Saturation Conditions
*	Effective value

## **4.2. PEMFC DYNAMIC MODEL DEVELOPMENT**

Due to some voltage drops, the fuel cell output voltage is lower than internal voltage that developed into FC. Voltage drops of a PEMFC diagram, and the voltage drops across it, from the anode gas through flow channel to the cathode is illustrated in Figure 4.1. The Ohmic voltage drops associated with the anode, cathode, and membrane at certain operating point can be considered as a linear function of thickness of those segments (Figure 4.1). During the energy barrier, the active voltage may decreasing. The reacting species should be overcome in chemical reactions inside FC.

It can be considered as an extra voltage necessary to enable the chemical reaction to proceed at a desired rate. The mass transfer processes lead to concentration voltage drop from bulk channels to reaction sites in porous electrodes, the concentration voltage drop will be significant under high current density, since the reactant concentration could be much less than the bulk of the gas stream. The concentration voltage drop may be neglected for low current densities [33].

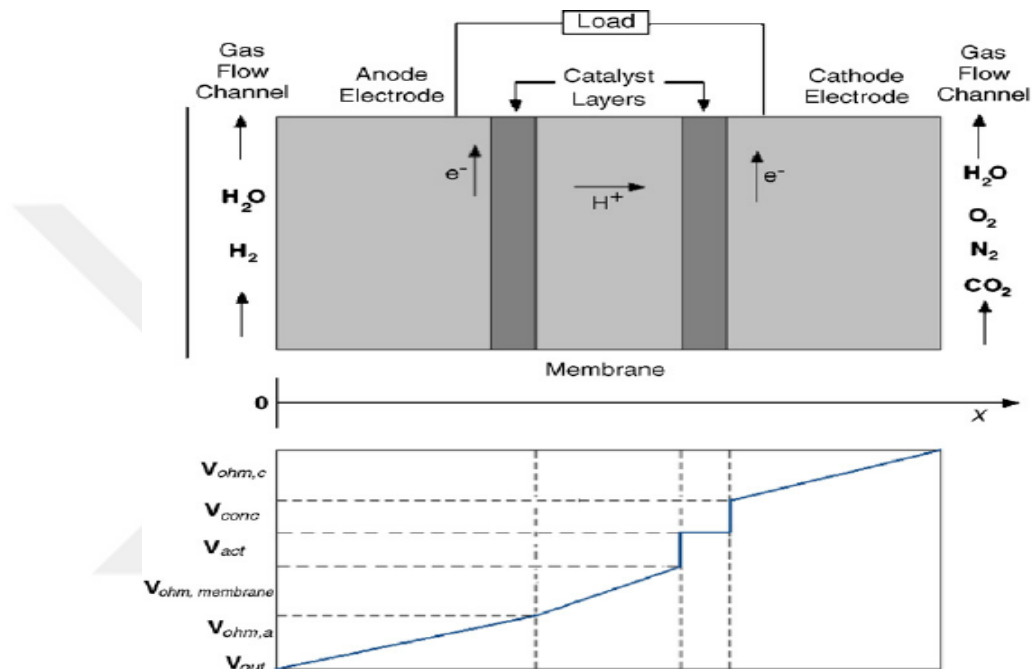


Figure 4.1. Voltage drops of a PEMFC diagram [33].

As following subsections, gas diffusion as function of position (x) across PEMFC (from anode to cathode) and dynamics of flow of hydrogen and oxygen in the electrode channels are derived. It will be shown that these quantities will lead to the development of the internal voltage and voltage drops inside PEMFC.

The following assumptions are also used here to simplify the analysis:

- (1) One-dimensional of gas treatment flow and distribution of species inside PEMFC.
- (2) Ideal and evenly distributed gas.
- (3) The fuel cell constant pressure in airflow path.
- (4) Fuel is humidifying hydrogen, oxidant is humidifying air.

- (5) The effective side of the anode side of the water vapor pressure of 50%, the cathode side of the saturated vapor pressure.
- (6) PEMFC is run at 100<sup>0</sup>C and the liquid phase of reaction.
- (7) Assess the thermodynamic properties at the average stack temperature, ignoring the temperature change in the stack, and assume that the overall specific heat capacity of the stack is constant.
- (8) The parameters of the individual cells are concentrated together to represent the fuel cell stack [33].

### 4.3. GAS DIFFUSION IN THE ELECTRODES

Determining the effective partial of pressures of H<sub>2</sub> and O<sub>2</sub>, in order to calculate the output voltage of Fuel Cell. The porous electrodes can be describe by the Stefan Maxwell formula in gas mix true consisted of N species and the diffusion of component i through [31].

$$\nabla \chi_i = \frac{RT}{P} \sum_{j=1}^N \frac{\chi_i N_j - \chi_j N_i}{D_{i,j}} \quad (4.1)$$

Normally, the gas is a mixture in the anode side of H<sub>2</sub> and H<sub>2</sub>O. In gas phase, the molar flux of water normal to anode surface N<sub>H<sub>2</sub>O</sub>, which can be setting to zero, according to the assumptions (1) – (3) the water diffusion calculated with formula:

$$\begin{aligned} \frac{dx_{H_2O}}{dx} &= \frac{RT}{Pa} \left( \frac{x_{H_2O} N_{H_2} - x_{H_2} N_{H_2O}}{D_{H_2O,H_2}} \right) = \\ &= \frac{RT}{Pa} \left( \frac{x_{H_2O} N_{H_2}}{D_{H_2O,H_2}} \right). \end{aligned} \quad (4.2)$$

We can calculate molar flux of H<sub>2</sub> by Faraday's Law [39]

$$N_{H_2} = \frac{I_{den}}{2F} \quad (4.3)$$

Equations (4.2) and (4.3) combined and integrated the expression with respect to from the anode to the catalyst surface will be:

$$x_{H_2O}^* = x_{H_2O}^{channel} \exp\left(\frac{RTI_{den}I_a}{2FP_aD_{H_2O,H_2}}\right) \quad (4.4)$$

According to the assumption (4)  $x_{H_2O}^* + x_{H_2}^* = 1$ , the effective partial pressure of H<sub>2</sub> is

$$P_{H_2}^* = \frac{P_{H_2O}^*}{x_{H_2O}^*} (1 - x_{H_2O}^*) \quad (4.5)$$

$P_{H_2}^*$  at the anode is  $0.5P_{H_2O}^{sat}$ . Therefore,  $P_{H_2}^*$  is given as

$$P_{H_2}^* = 0.5P_{H_2O}^{sat} \left[ \frac{1}{x_{H_2O}^{channel} \exp\left(\frac{RTI_{den}I_a}{2FP_aD_{H_2O,H_2}}\right)} - 1 \right] \quad (4.6)$$

In the cathode channel gases flowing are O<sub>2</sub>, N<sub>2</sub>, O<sub>g</sub> and CO<sub>2</sub>. Using equation (4.1) the diffusion of H<sub>2</sub>O<sub>g</sub> can be obtained from the cathode side:

$$\frac{dx_{H_2O}}{dx} = \frac{RT}{P_C} \left( \frac{x_{O_2}N_{H_2O} - x_{H_2O}N_{O_2}}{D_{H_2O,O_2}} \right) \quad (4.7)$$

$P_C$ —the overall gas pressure at the cathode (Pa).

$$\frac{RT}{P_C} = \left( \frac{-x_{H_2O}N_{O_2}}{D_{H_2O,O_2}} \right) \quad (4.8)$$

As same as the anode, can be calculated the effective molar fraction of water at the cathode catalyst interface with equation:

$$x_{H_2O}^* = x_{H_2O}^{channel} \exp\left(\frac{RTI_{den}l_c}{4FP_C D_{H_2O,O_2}}\right) \quad (4.9)$$

Through similar analytical procedures [(4.7), (4.8)], the effective molar fraction of  $N_2$  and  $CO_2$  will know as:

$$x_{N_2}^* = x_{CO_2}^{channel} \exp\left(\frac{RTI_{den}l_c}{4FP_C D_{N_2,O_2}}\right) \quad (4.10)$$

$$x_{CO_2}^* = x_{CO_2}^{channel} \exp\left(\frac{RTI_{den}l_c}{4FP_C D_{CO_2,O_2}}\right) \quad (4.11)$$

The effective molar fraction of  $O_2$  is

$$x_{O_2}^* = 1 - x_{H_2O}^* - x_{N_2}^* - x_{CO_2}^* \quad (4.12)$$

Effective partial pressure of  $O_2$  is

$$P_{O_2}^* = \frac{P_{H_2O}^*}{x_{H_2O}^*} x_{O_2}^* = \frac{P_{H_2O}^*}{x_{H_2O}^*} (1 - x_{H_2O}^* - x_{N_2}^* - x_{CO_2}^*) \quad (4.13)$$

According to assumption (5) the equation (4.13) is rewritten as follows

$$P_{O_2}^* = P_{H_2O}^{sat} \left[ \frac{1 - x_{N_2}^* - x_{CO_2}^*}{x_{H_2O}^*} - 1 \right] \quad (4.14)$$

From equations (4.6) and (4.14)  $P_{H_2}^*$  and  $P_{O_2}^*$  can be calculated and using in the Nernst equation to find the fuel-cell output voltage.

#### 4.4. PEMFC MODEL STRUCTURE

A computer model can be developed for PEMFC based on its thermodynamic and electrochemical properties, to predict the fuel cell dynamic response. The output voltage of FC depends on the temperature and load current. Since the fuel cell.

Operation temperature and output voltage across the equivalent capacitance of double-layer charge effect are a function of time during a transient state, the resultant output voltage of fuel cell is a dynamic quantity.

Using block diagram Figure 4.2 we will develop computer model showing for PEMFC. The input parameters of PEMFC are: anode and cathode pressures, the initial fuel cell temperature, and room temperature. So, the internal temperature  $T$  will determine from feedback variables of load current and time and involved in determination of output voltage of PEMFC [31,34].

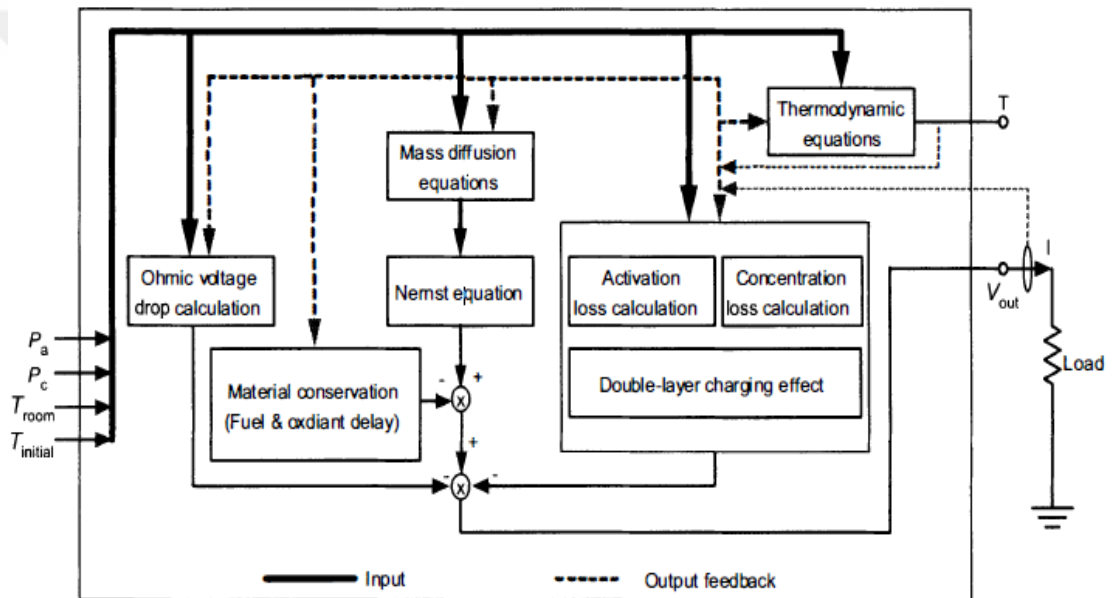


Figure 4.2. Block diagram of PEMFC [37].

#### 4.5.EQUIVALENT ELECTRICAL CIRCUIT MODEL OF PEMFC

The fuel cell typically operates with another electrical equipment, like a power electronic interface circuit (converter), which converts the DC output voltage of the variable fuel cell into a controllable AC voltage. Thus, the equivalent circuit model of the fuel cell can be a valuable tool for use with the circuit model of the interface component to study the performance of the fuel cell power generation system. Using block diagram of PEMFC Figure 4.3 we will build electric circuit. The block diagram consists of the following blocks: internal potential, activation, concentration,

ohmic and thermodynamic blocks.  $C$  is the capacity of the double-layer charge effect [33, 37].

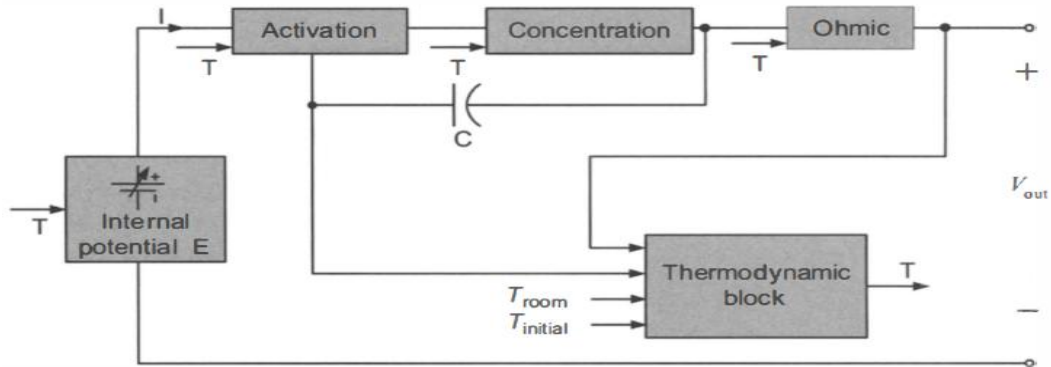


Figure 4.3. Block diagram of PEMFC to build electrical circuit [37].

#### Equivalent Circuit for the Internal Potential Block

The internal potential fuel cell  $E$  is function of the load current and temperature. The equivalent circuit for internal potential ( $E$ ) is illustrated in Figure 4.4, where input is standard potential  $E_0^o$ ,  $T = 298 \text{ K}$ ,  $P = 1 \text{ atm}$ , and its output is stack internal potential  $E$  of PEMFC. From Figure 4.4 internal potential  $E$  of electrical circuit equals:

$$E = E_0^o - f_1(I, T) - f_2(I) \quad (4.15)$$

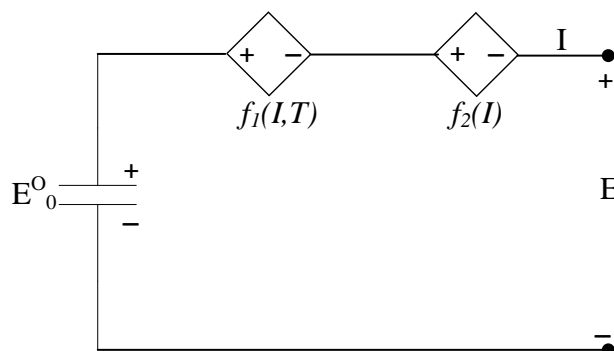


Figure 4.4. The equivalent circuit for internal potential  $E$ .

#### Equivalent circuit for the activation

Activation voltage drop equation can be written as sum of  $V_{act1}$  and  $V_{act2}$  :

$$V_{act} = \eta_0 + (T - 298) \cdot a + T \cdot b \cdot \ln(I) = V_{act1} + V_{act2} \quad (4.16)$$

where:  $\eta_0, a, b$ —empirical constants.

$V_{act1} = (\eta_0 + (T - 298)a$  – voltage drop that affect by the fuel cell internal temperature (is not current depenent).

$V_{act2} = (T \cdot b \cdot \ln(I))$  – voltage drop that depended on current and temperature.

$V_{act1}$  can be modeled by constant voltage source in series with a temperature-controlled voltage source.  $V_{act2}$  can be modeled by voltage drop across a temperature and currentdependent resistor  $R_{act}$

$$R_{act} = V_{act2} / I = T \cdot b \ln(I) / I \quad (4.17)$$

This resistor comprises of a fixed resistor  $R_{act0}$ , a current-dependent resistor ( $R_{Aact1}(I)$ ) and a current and temperaturedependent resistor ( $R_{Aact2}(I., T)$ ). A current dependent resistor can be built, by using a polynomial current-controlled voltage source model.

From Figure 4.5 an electrical equivalent circuit for activation voltage drop is shown we can write equationsfor  $V_{act1}$  and  $V_{act2}$ .

$$V_{act1} = \eta_0 + f_3(T) = \eta_0 + (T - 298)a \quad (4.18)$$

$$V_{act2} = (R_{act})(I) = (R_{act0} + R_{act1} + R_{act2})(I) \quad (4.19)$$

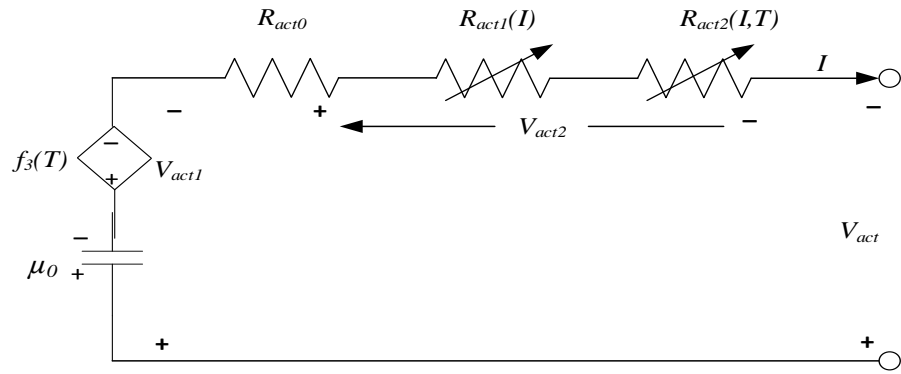


Figure 4.5. Activation loss of electrical circuit model in PEMFC.

### Equivalent circuit for the ohmic voltage drop

Equivalent electrical circuit for the fuel cell ohmic voltage drop shown in Figure 4.6,

$R_{ohm}$  is function of current and temperature. From Figure 4.6 we have

$$R_{ohm} = R_{ohm0} + k_{RI}I - k_{RT}T \quad (4.20)$$

where:  $R_{ohm0}$  – the constant part of  $R_{ohm}$ ,

$k_{RI}$  – the empirical constant for calculating  $R_{ohm}(\Omega/A)$ ,

$k_{RT}$  – the empirical constant for calculating  $R_{ohm}$ .

So,  $R_{ohm}$  is given by

$$R_{ohm} = R_{ohm0} + R_{ohm1} + R_{ohm2} \quad (4.21)$$

where:  $R_{ohm0}$  – the constant part of  $R_{ohm}$  with reference to equation (4.20)

$R_{ohm1} = k_{RI}I$  – the current depending part of  $R_{ohm}$ ,

$R_{ohm2} = k_{RT}T$  – temperature depending part of  $R_{ohm}$ .

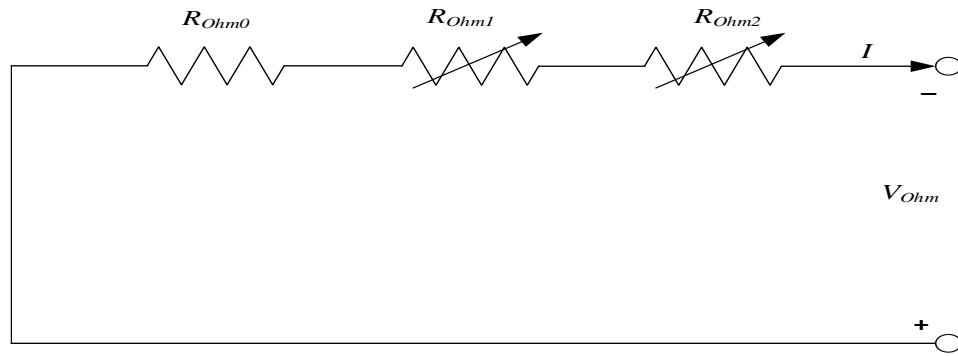


Figure 4.6. Electrical circuit model of ohmic voltage drop in PEMFC.

### Equivalent Circuit for Concentration Voltage Drop

According to Fick's first law and Faraday's law the equivalent resistance for concentration loss [39]:

$$R_{conc} = \frac{V_{conc}}{I} = -\frac{RT}{zFI} \ln\left(1 - \frac{I}{I_{limit}}\right) \quad (4.22)$$

Using Figure 4.7 and equation (4.22) the concentration equivalent resistance can be defined

$$R_{conc} = \frac{V_{conc}}{I} = R_{conc0} + R_{conc1} + R_{conc2} \quad (4.23)$$

where:  $R_{conc0}$  – the constant part of  $R_{conc}$ ,

$R_{conc1}$ ,  $R_{conc2}$  – both current and temperature are dependent parts of  $R_{conc}$ .

There is no voltage source in the equivalent circuits for the ohmic and concentration voltage drops since there is no generation associated with these circuits. They strictly represent voltage drops.

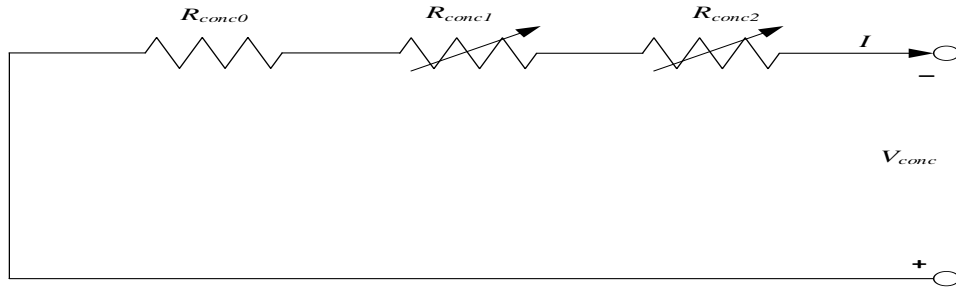


Figure 4.7. Concentration voltage drop circuit for PEMFC.

### Circuit Model for the Thermodynamic Block

The thermodynamic equivalent circuit model for PEMFC is developed using the analogies between thermodynamic and electrical parameters Table 4.1. The equivalent electrical circuit of thermodynamic model of PEMFC is given in Figure 4.8. According to the chemical reaction inside the fuel cell the net heat generation rate can be written as:

$$q_{net}^- = q_{chem}^- - q_{elec}^- - q_{sens}^- + latent - q_{loss}^- \quad (4.24)$$

where:  $q_{net}^-$  – the net heat energy (J) .

$q_{chem}^-$  –the chemical energy (J) .

$q_{elec}^-$  –the electrical energy (J) .

$q_{sens}^- + latent$  –the sensible and latent heat (J).

$q_{loss}^-$  – the heat loss (J).

The fuel cell operates at constant temperature at steady state and  $\overline{q_{net}} = 0$ . During transitions, fuel cell temperature will rise or drop according to the fuel cell specific heat capacity and its net heat rate as follows

$$M_{FC} C_{FC} \frac{dt}{dt} = q_{net}^- \quad (4.25).$$

where:  $M_{FC}$  – the total mass of the fuel stack;

$C_{FC}$  –the overall specific heat capacity of the stack.

Table 4.1. Analogies between electrical and thermodynamic parameters.

Electrical potential $U(V)$	Temperature $T(K)$
Electrical current $I(A)$	Heat flow rate $P_h(w)$
Electrical resistance $R(ohm)$	Thermal resistance $\theta(K/W)$
Electrical capacitance $C(F)$	Heat capacity $C_h(J/K)$
$RI = U$	$\theta P_h = T$
$I = C \frac{dU}{dt}$	$P_h = C_h \frac{dT}{dt}$

The equations (4.24) – (4.25) can be expressed by the R – C circuit Figure 4.8.

In fact, the power that consuming by the activations, ohmic and concentration losses equals  $(E - V_{OUT}) \times I$ . The rate of change of the heat source is:

$$q_{in}^* = (E - V_{OUT}) \times I \quad (4.26)$$

The thermal resistance according to air convection in the fuel cell:

$$R_T = \frac{1}{h_{cell} * N_{cell} * A_{cell}} \quad (4.27)$$

where:  $h_{cell}$  – the convective heat transfer coefficient  $(W/(m^2 K))$ .

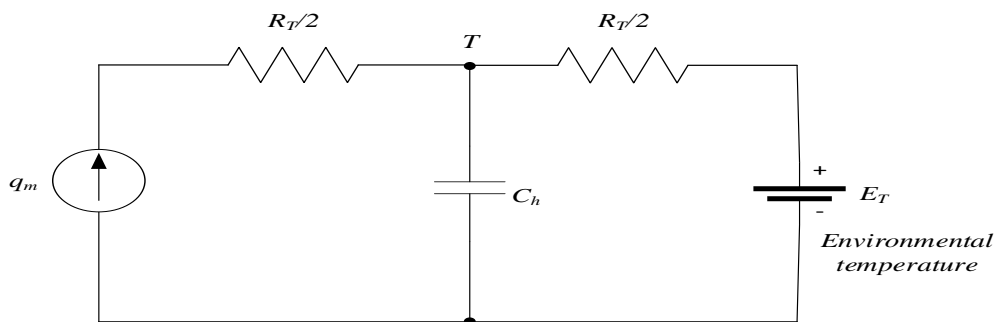


Figure 4.8. Equivalent electric circuit of thermodynamic model for PEMFC.

## CHAPTER 5

### MODELLING AND SIMULATION OF SR-12 PEM FUEL CELL ON MATLAB/SIMULINK

In chapter 4, we considered the main equations and the equivalent electrical circuits of PEM fuel cell. Using these dynamic models and equations for PEM fuel cell specification of SR-12 model of PEM fuel cell simulation models are developed on MATLAB/SIMULINK environment.

#### 5.1.SPECIFICATIONS OF SR-12 PEMFC

The Input Parameters of SR-12 PEM Fuel Cell are following:

- Fuel cell maximum load current I: 24 A.
- Channel pressure at anode P: 1.5 (atm)
- Channel pressure at cathode P: 1.0 (atm)
- Room temperature T: 307.7 K
- Initial temperature of FC T: 307.7 K

The Output Parameters of SR-12 PEM Fuel Cell are following:

- Output terminal voltage V:
- FC power (W) output P.
- Temperature (K) output T.

Proper simulation time needs to be set before simulation. Simulation time is determined by the length of simulation study desired and/or the length of the actual input data. Electrical parameters of SR-12 PEMFC which are used to built simulation model of PEMFC are given in Table 5.1.

Table 5.1. Electrical parameters of SR-12 PEMFC.

Name	Value	Name	Value
$E_0 (V)$	$1.229 * N_{CELL} V$	$V_{CONC} (V)$	0.085
	80	$V_{OHMIC} (V)$	0.13
$E_{CELL} (V)$	$1.216 * N_{CELL} V$	$N_{CELL}$	48
$E_{d,cell} (V)$	$0.062V$	$A_{CELL}$	$3.2e^{-2}$
$\lambda_e (\Omega)$	$0.00333\Omega$	$M_{FC} C_{FC}$	$2.2e^4$
$\Delta G_0 (J / m_0)$	$273e^{-3}$	$C_h (F)$	2200
$\eta_0 (V)$	20.145	$C (F)$	4
$a (V / K)$	0.1373	$RT (\Omega)$	0.0347
$\Delta G (J / m_0)$	$2.355e^5$	$R_{act0} (\Omega)$	1.2581
$New\Delta G_0 (J / m_0)$	$(T - T_0) * 0.163$	$R_{act2} (\Omega)$	$0.00112 * (T - 298)$
$V_{ACT1} (V)$	0.36	$R_{ACT} (\Omega)$	$R_{ACT0} + R_{ACT1} + R_{ACT2}$
$V_{ACT2} (V)$	0.099	$R_{OHMIC0} (\Omega)$	0.2793
$V_c (V)$	0.18	$R_{ohmic1} (\Omega)$	$0.001872 * I$
$R_{CONC} (\Omega)$	$R_{conc0} + R_{concl} + R_{conc2}$	$R_{conc0} (\Omega)$	0.080312
$R_{ohmic} (\Omega)$	$R_{ohmic0} + R_{ohmic1} + R_{ohmic2}$	$R_{ohmic2} (\Omega)$	$-0.0023712 * (T - 298)$
$R_{concl} (\Omega)$	$5.2211e^{-8} I^6 - 3.4578e^{-6} I^5 - 8.6437e^{-5} I^4 - 0.010089 I^3 + 0.005554 I^2 - 0.010542 I$	$R_{conc2}$	$0.0002747 * (T - 298)$
$R_{act1} (\Omega)$	$-1.6777e^{-6} I^5 + 1.2232e^{-4} I^4 - 3.4e^{-3} I^3 + 0.04545 I^2 - 0.3116 I$	$h_{cell}$	37.5

Using electrical parameters, we developed simulation model of SR-12 PEMFC on MATLAB/Simulink Figure 5.1.

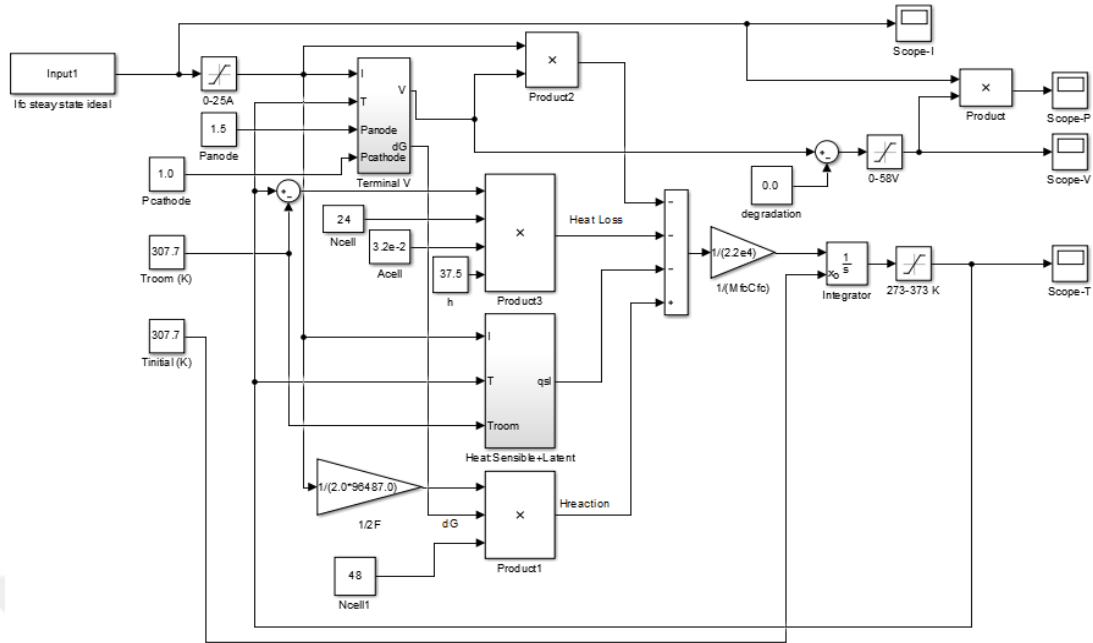


Figure 5.1. Model of SR-12PEMFC on MATLAB/Simulink.

Table 5.2. Specification of SR-12 PEMFC is presented.

Description	Value
Capacity	500 W
Number of cells N	48
Cell area A	320 cm <sup>2</sup>
Operating environmental temperature	5 – 30 °C
Weight	44 kg

## 5.2. MODELLING OF PEMFC BLOCKS

The model Active pressure of gas diffusion at electrodes on MATLAB/Simulink shows in the Figure 5.2. We assume that  $P$  anode and  $P$  cathode are constant.

The output of active pressures  $P_{H_2}^*$  and  $P_{O_2}^*$  we can calculate according to the equations (4.6) and (4.14):

$$\text{So, } P_{H_2}^* = 1 \text{ atm}$$

So,  $P_{O_2}^* = 1 \text{ atm}$

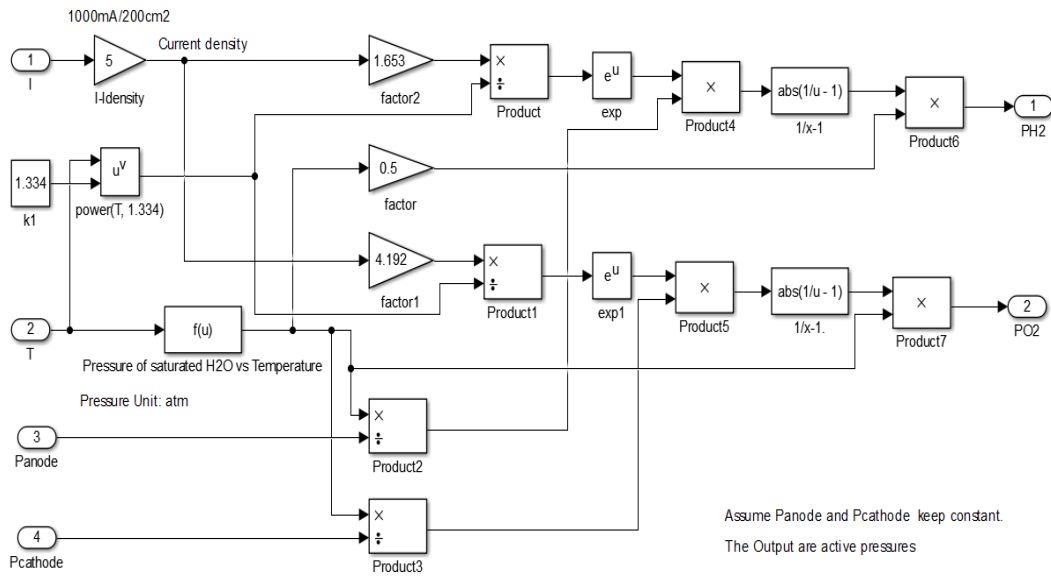


Figure 5.2. The model Active pressure of gas diffusion at electrodes on MATLAB/Simulink.

The internal potential,  $E_{cell}$  we can calculate from the following equation.

$$E_{cell} = E_0 + \frac{RT}{2F} \ln \left[ p_{H_2}^* \cdot (p_{O_2}^*)^{0.5} \right] E_{d.cell} \quad (5.1)$$

where: the product given us  $\ln [P_{H_2} \cdot (P_{O_2})^{0.5}]$ ,

$$\text{The Product4} = \frac{RT}{2F},$$

$$\frac{R}{2F} = 4.3085 * 10^{-5},$$

$$E_{d.cell} = 0.062 \text{ V},$$

$$\text{So, } E_{cell} = 1.216 \text{ V}$$

So we can find the Fuel Cell efficiency according to (3.20)  $\eta = 0.8208$

According to the equation (3.14) we write gas Gibbs free energy  $\Delta G$ .

$$\Delta G = \Delta G_0 + \Delta G_1(RT \ln (p_{H_2} \cdot P_{O_2}^{0.5})) \quad (5.2)$$

where:  $R = 8.31 \text{ } \Omega$ ,  $\Delta G_0 = 237.2 * 10^{-3} \text{ J} / M_0$

so,  $\Delta G = 2.355 * 10^5 \text{ J} / M_0$

The developed model of internal potential voltage  $E_{cell}$  and  $\Delta G$  on Matlab/Simulink shown in Figure 5.3.

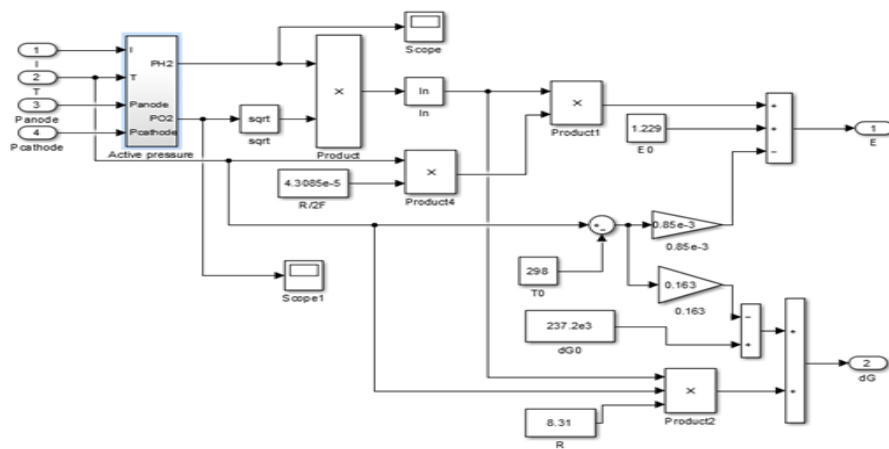


Figure 5.3. The model of internal potential voltage  $E_{cell}$  and  $\Delta G$  on MATLAB/Simulink.

After that we build the simulation model of ohmic voltage drop Figure 5.4. According to the equation (4.20), we can write the ohmic voltage drop.

$$v_{OHMIC} = I * R_{ohmic} \quad (5.3)$$

So,  $v_{OHMIC} = 0.13 \text{ V}$ .

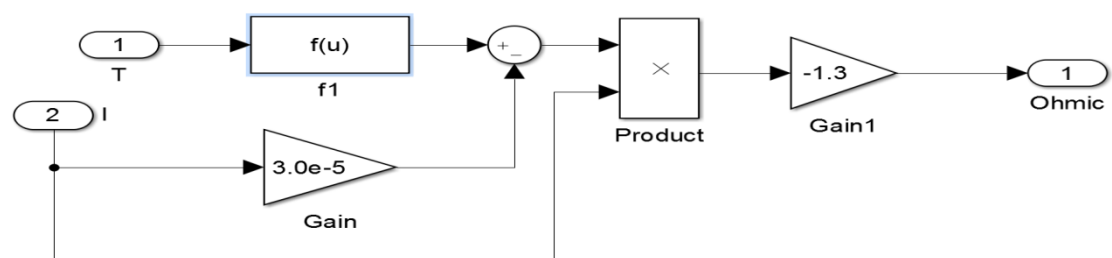


Figure 5.4. The model of ohmic voltage drop on MATLAB/Simulink.

The model of concentration voltage drop on MATLAB/Simulink is illustrated in Figure 5.5. According to the equations (4.23), (4.24) and assuming  $\frac{R}{2F} = 4.3085 \times 10^{-5}$ , fuel cell current limit  $I_{limit} = 1$  (mA), we have  $V_{CONC} = 0.085$  V

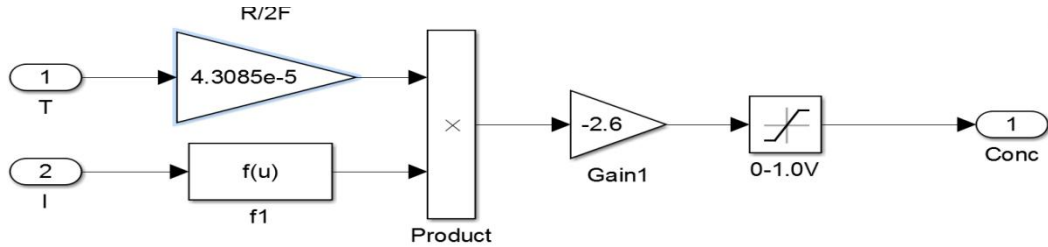


Figure 5.5. The Model of concentration voltage drop on MATLAB/Simulink.

The model of activation voltage drop1 on MATLAB/Simulink shown in Figure 5.6, We have calculated  $V_{Act1}$  according to the equation (4.19), where:  $\eta_0 = 20.145$ .

a – Empirical constants. So,  $V_{Act1} = 0.36$  V . Activation voltage drop 1  $V_{act1}$  effects just with internal temperature of fuel cell (is not current dependent).

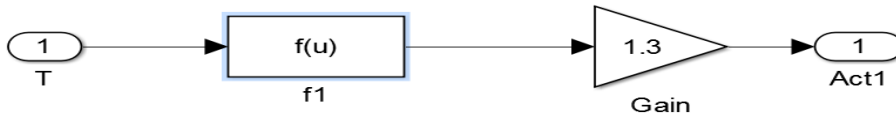


Figure 5.6. The model of activation voltage drop1 on MATLAB/Simulink.

Therefore, the model of activation voltage drop 2 on MATLAB/Simulink shown in Figure 5.7. According to the equation (4.20), we have  $V_{act2} = 0.099$  V , where:  $b$ – empirical constant.

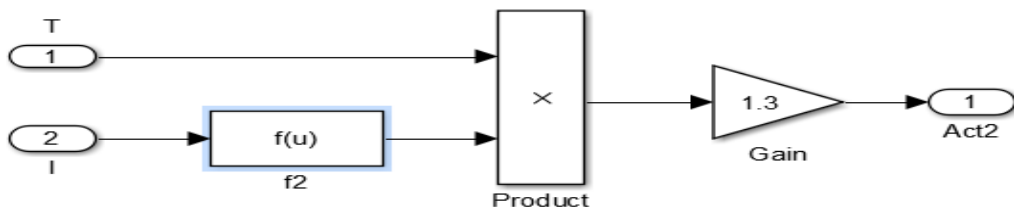


Figure 5.7. The model of activation voltage drops 2 on MATLAB/Simulink.

The model of drop delays block on MATLAB/Simulink is illustrated in Figure 5.8, The overall effect of fuel and oxidant delays is appeared as voltage  $E_{d,cell}$ , which is subtracted from the right side the fuel and oxidant delays on the fuel cell output voltage during load transients we can calculate as:

$$E_{d,cell} = \lambda_e I_{(s)} \frac{1}{\tau_e + 1} \quad (5.4)$$

where:

$\lambda_e$ —constant value,  $\lambda_e = 0.0033\Omega$ ;

$\tau_e$ —overall flow delay (s),  $\tau_e = 80$ .

So,  $E_{d,cell} = 0.062 \text{ V}$

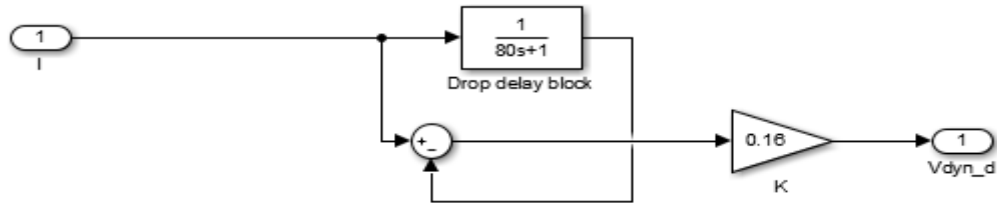


Figure 5.8. The model of drop delays block on MATLAB/Simulink.

In a PEMFC, the solid membrane blocks the electron flow and allow passing only hydrogen protons. Electrochemical double layer stores electrical (Figure 5.9).  $R_{act}$  can be defined as follows:

$$R_{act} = \frac{V_{act2}}{I} = \frac{T.b \ln(I)}{I} \quad (5.5)$$

Internal voltage is defined as  $E - V_{act1}$ . Activation drop voltage 1  $V_{act1}$  is the temperature-dependent part of  $V_{act}$ .  $R_{conc}$  is the equivalent resistance of concentration voltage drop equals to the following:

$$R_{conc} = \frac{V_{conc}}{I} = \frac{RT}{zFI} \ln\left(\frac{I}{I_{limit}}\right) \quad (5.6)$$

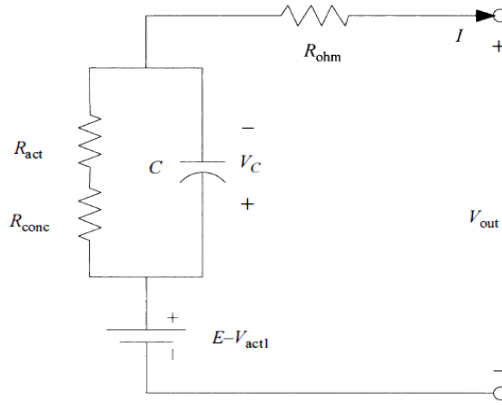


Figure 5.9. Equivalent circuit of the double-layer charge effect inside within PEMFC.

The voltage  $V_C$  across  $C$  can be write as follows:

$$V_C = (I - C \frac{dV_C}{dt})(R_{act} + R_{conc}) \quad (5.7)$$

$$(I - C \frac{dV_C}{dt}) = \frac{V_C}{(R_{act} + R_{conc})} \quad (5.8)$$

$$(C \frac{dV_C}{dt}) = I - \frac{V_C}{(R_{act} + R_{conc})} = (\frac{dV_C}{dt}) = \frac{I}{C} - \frac{V_C}{(R_{act} + R_{conc})} = \quad (5.9)$$

$$V_C = \int \frac{1}{C} (I - \frac{V_C}{R_{act} + R_{conc}}) dt$$

where:  $C = 4F$

So, after calculation we have  $V_C = 0.18 V$ .

The model of terminal voltage on MATLAB/SIMULINK is given in Figure 5.10. The integration in the modeling can be effected by double-layer charge by using  $V_C$  for calculating  $V_{out}$ . From Figure 5.9 we write the fuel cell output voltage:

$$V_{out} = E - V_{act1} - V_C - V_{ohm} \quad (5.10)$$

$$V_{out} = 0.503 \times N_{cell} = 24.144V$$

where:  $N_{cell} = 48$ .

The Activation phenomenon has been considered by two parts: *Activation1* and *Activation2*.

The  $Act_1$  is temperature dependent voltage drop. The  $Act_2$  is the temperature and current dependent voltage drop. However, it has been converted into an equivalent resistance first, and then it will be combined together with  $R_{conc}$ , and the capacitor due to double-layer change effect to give the voltage drop  $V_{C1}$ . The electrical output power equals:

$$q = V_{OUT} * I = 580 \text{ W} \quad (5.11)$$

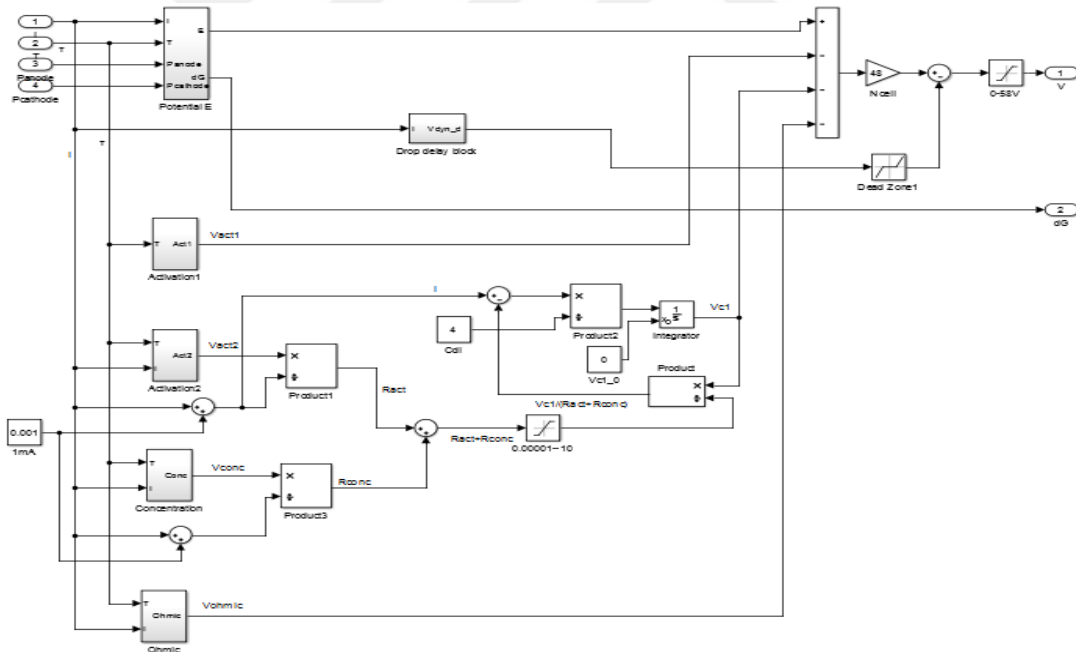


Figure 5.10. The model of terminal voltage on MATLAB/SIMULINK.

We also developed sensible and latent head models on MATLAB/Simulink (Figure 5.11). Sensible heat is intended to transform heat energy by a body that has a temperature higher than its surrounding. During a change of state or phase, the energy that resulted in form of heat named as Latent heat. Assuming that inlet

temperature is equals to room temperature the sum of two heats can be written as follows:

$$q_{sens} + q_{latent} = (n_{H_2} \times C_{H_2} \times (T - T_{room})) + (n_{O_2} \times C_{O_2} \times (T - T_{room})) + n_{H_2} \times C_{H_2O} \times (T - T_{room}) + n_{H_2O} \times H_V \quad (5.12)$$

And using values of  $n_{H_2} = \frac{1}{2f} I$ ,  $n_{O_2} = \frac{1}{4f}$ ,  $n_{H_2O} = \frac{1}{2f}$ ,  $H_V = 40644$  we calculate

$$q_{sens} + q_{latent} = 300 \text{ J}$$

Heat loss estimated as follows

$$q_{loss} = (h_{cell}) (N_{cell}) (A_{cell}) (T - T_{room}) \quad (5.13)$$

$$\text{So, } q_{loss} = 325 \text{ J}$$

where:  $h_{cell}$  – the convective heat transfer coefficient  $W / m^2 K = 37.5$ ,  $N_{cell} = 24$ , and  $A_{cell} = 3.2 * 10^{-2}$ .

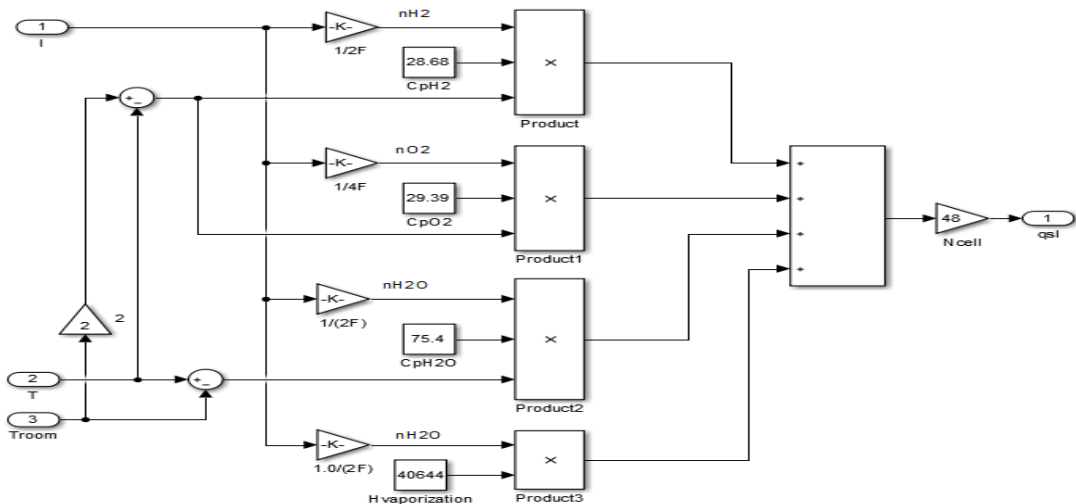


Figure 5.11. The model of Sensible + Latent Heat on MATLAB/Simulink.

Then we calculate the reaction heat:

$$q_{reaction} = (T - T_{room}) (n_{H_2O}) \times \Delta G \quad (5.14)$$

So,  $q_{reaction} = 1300 \text{ J}$

$$\text{where: } n_{H_2O} = \frac{1}{2f} = \frac{1}{2 * 96487.0}.$$

We also can calculate the temperature in Kelvin according to (4.24). If  $q_{net}^- = 111 \text{ J}$  temperature follows as:

$$T = q_{net}^- * \frac{1}{M_{FC} C_{FC}} \quad (5.15)$$

$$\text{So, } T = 317 \text{ K} . \text{ where: } \frac{1}{M_{FC} C_{FC}} = \frac{1}{2.2 * 10^4} ,$$

The total temperature equals:

$$T_{total} = \int T - T_{INITIAL} = 321 \text{ K} \quad (5.16)$$

We assume that the concentration potential cannot exceed 1.0 V for each individual cell.

### 5.3. RESULTS OF SIMULATION

In simulation results of PEM fuel cell current increases from 1 A up to 24 A in linear form (Figure 5.12).

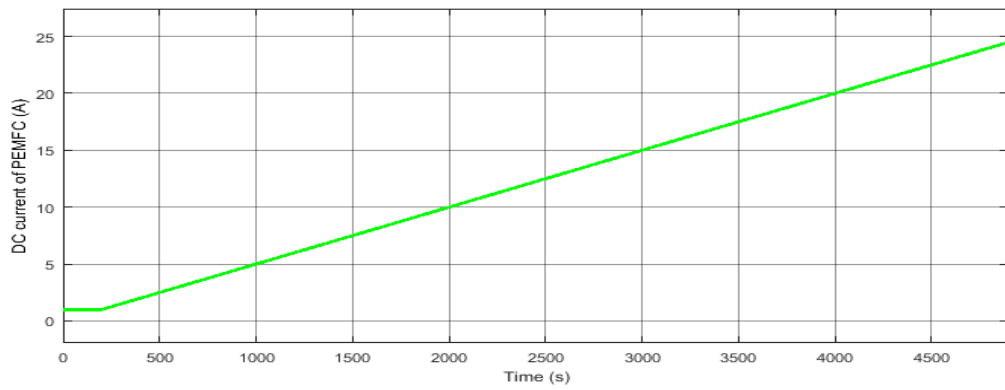


Figure 5.12. Simulation result of PEM fuel cell current.

Simulation result of PEMFC voltage shown in Figure 5.13. The voltage characteristics decreases from maximum 38 V until 24 V once time is taken 4500 sec.

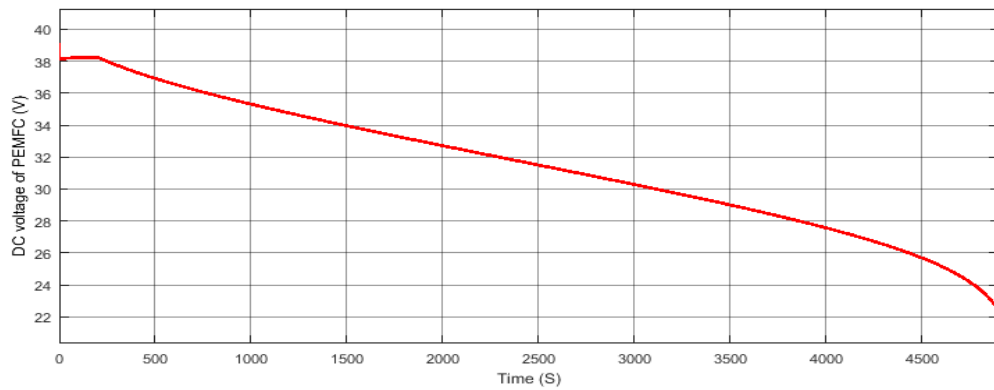


Figure 5.13. Simulation result of PEM fuel cell voltage.

Simulation result of PEMFC output power shown in Figure 5.14. The output power starts from 50 W and waveform of power increases until its maximum value 580 W for time 4500 sec.

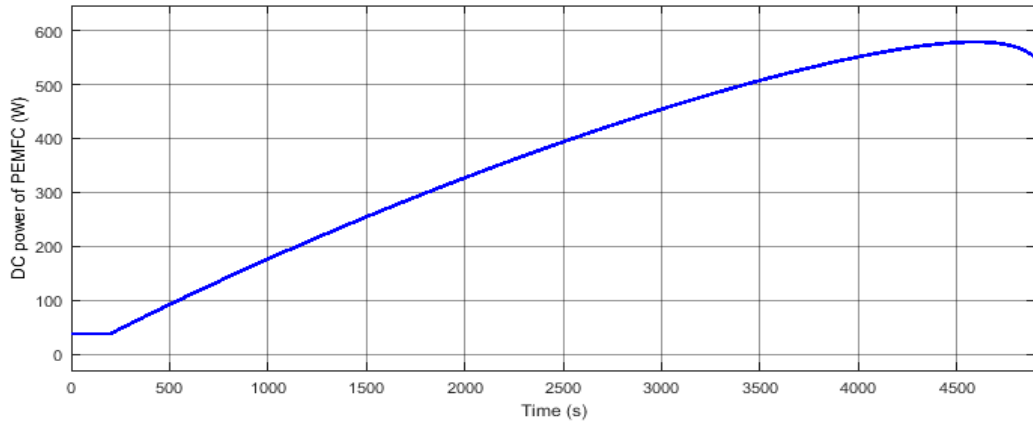


Figure 5.14. Simulation result of PEM Fuel Cell output power.

Simulation result of PEMFC output temperature shown Figure 5.15 PEMFC output temperature is nonlinear and varying on time that starts from 307 K and gets on its maximum value 321 K.

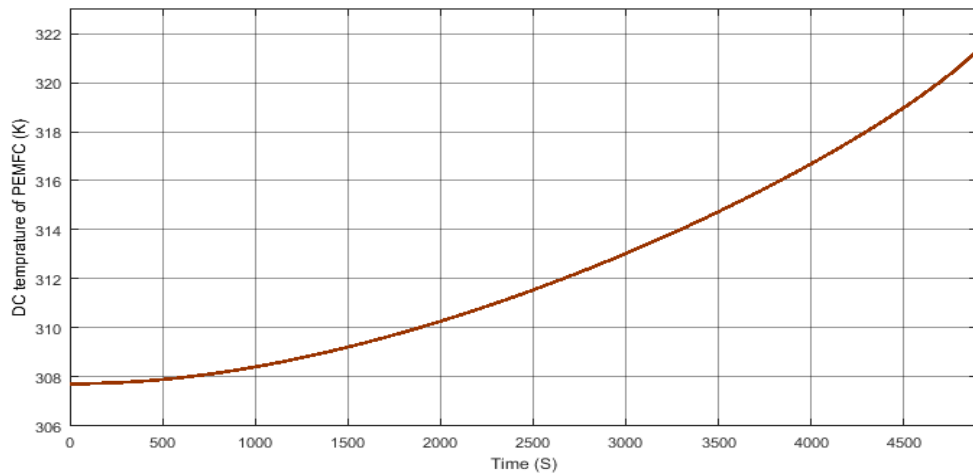


Figure 5.15. Simulation result of PEMFC output temperature.

We use DC/DC converter and DC/AC inverter for SR-12 PEM fuel cell model.

Block diagram of PEMFC – DC/DC converter – DC/AC inverter – Load system is illustrated in Figure 5.16. According to this block diagram, we firstly built simulation model of DC/DC converter on MATLAB/Simulink (Figure 5.17).

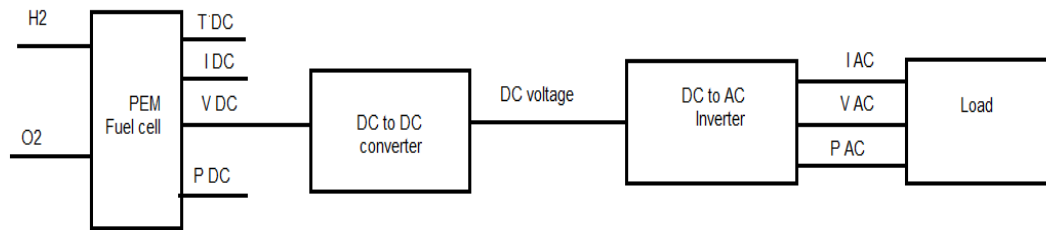


Figure 5.16. Block diagram of PEMFC – DC/DC converter – DC/AC inverter – Load system.

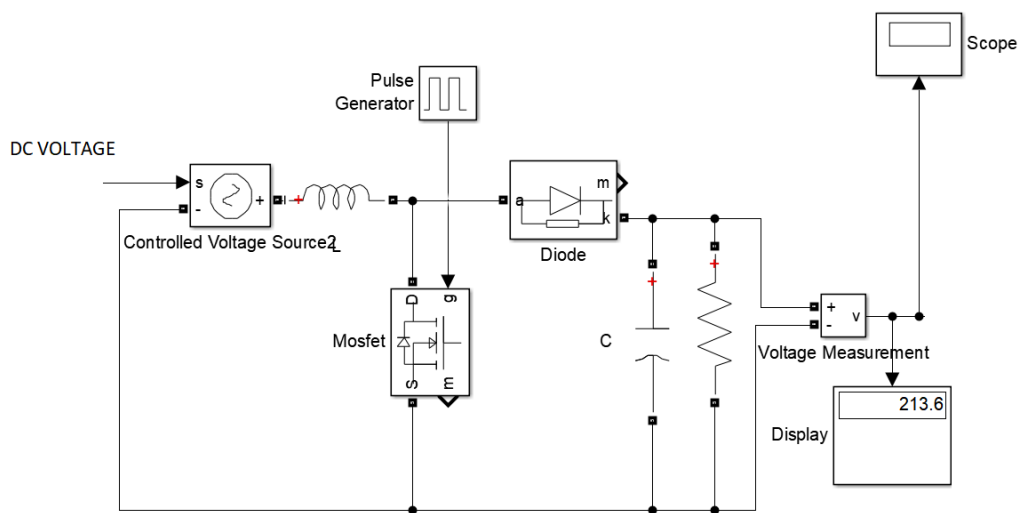


Figure 5.17. Simulation block of DC/DC converter on MATLAB/Simulink.

We can see that output voltage of DC/DC converter after approximately 0.01 sec takes its steady-state value of 220 V(Figure 5.18).

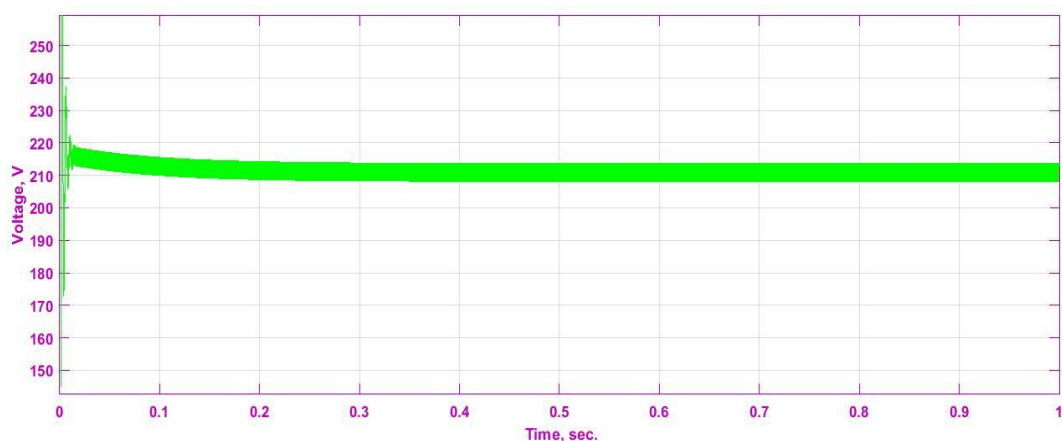


Figure 5.18. Voltage of DC/DC converter.

DC output voltage comes from DC/DC converter and inverts to AC voltage by DC/AC inverter. Simulation block of DC/AC inverter on MATLAB/Simulink is given in Figure 5.19.

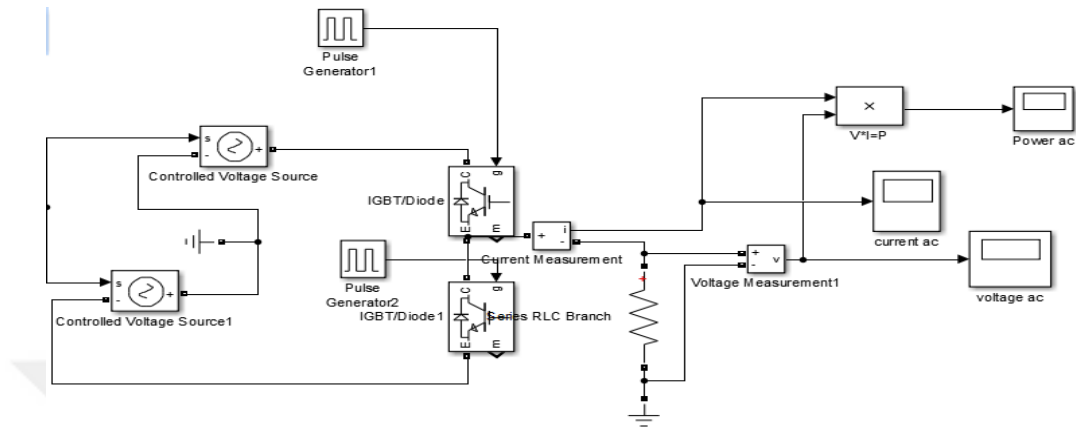


Figure 5.19. Simulation block of DC/AC inverter on MATLAB/Simulink.

Current and voltage results of DC/AC inverter are shown in Figures 5.20 and 5.21, respectively.

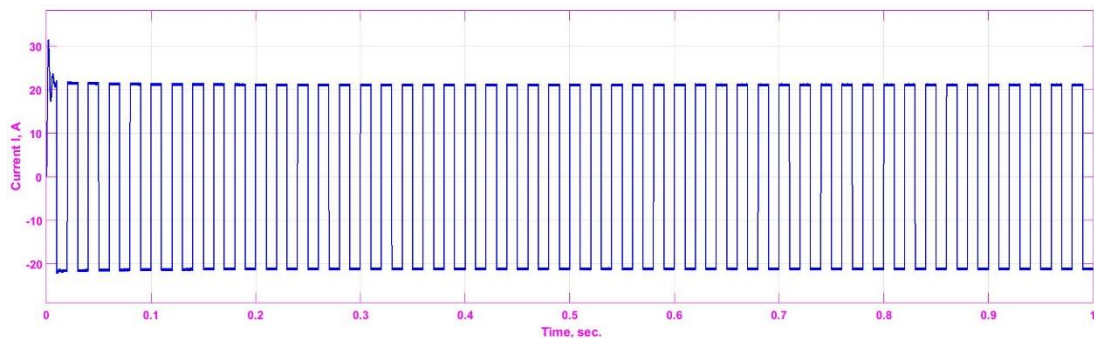


Figure 5.20. Current results of DC/AC inverter.

From Figure 5.20 we can see the instantaneous current of inverter is 39 A and steady-state value of current takes in 0.01 sec.

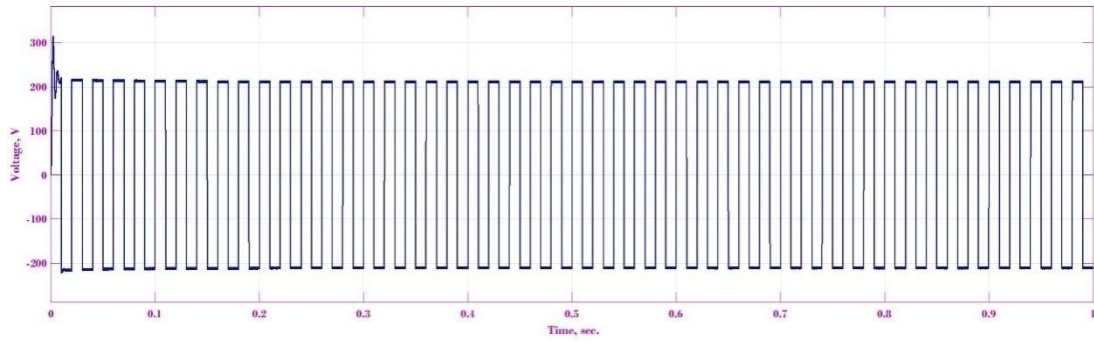


Figure 5.21. Voltage results of DC/AC inverter.

From Figure 5.21 we can see the output voltage of inverter reaches its stable value of 220 V at short time – 0.01 sec.

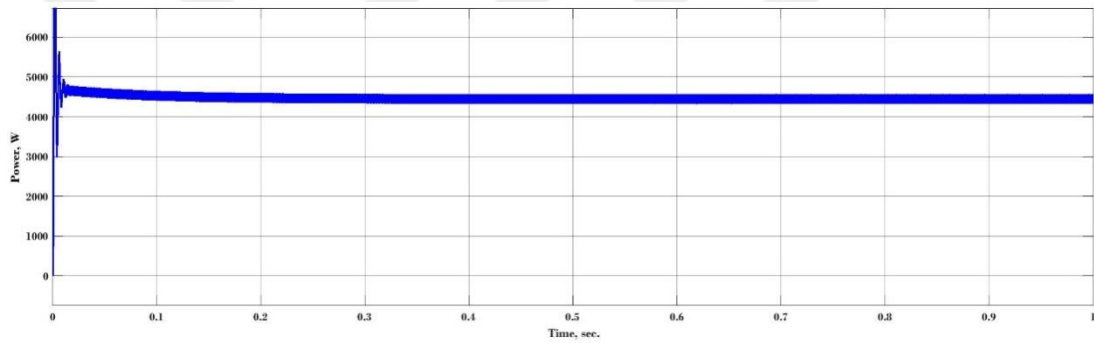


Figure 5.22.AC Power results of voltage inverter.

Power characteristics of DC/AC inverter presented in Figure 5.22. We can see that stable power of inverter reaches at 0.015 sec and equals to 4.5 kW.

Finally, developed Simulink model of SR-12 PEMFC on MATLAB/Simulink shown in Figure 5.23.

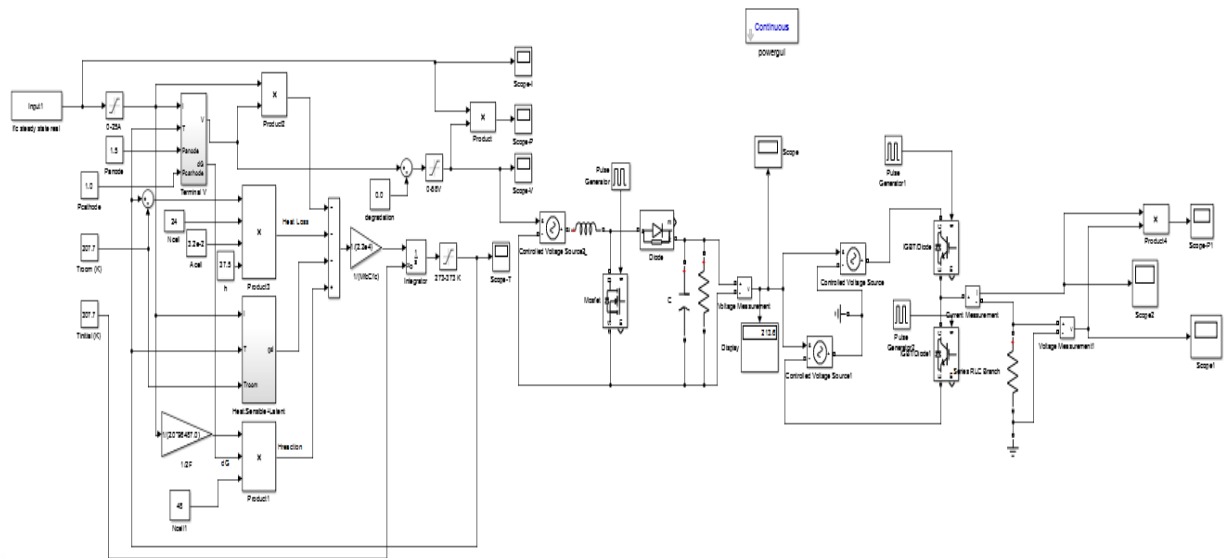


Figure 5.23. Simulink model of SR-12 PEMFC DC voltage in MATLAB/Simulink with converter and inverter to load.

#### 5.4. CONCLUSIONS AND FUTURE WORKS

Microgrid is the basic element and key component of Smart Grid. Microgrid is designed to improve energy efficiency, power system reliability and reduce carbon dioxide emissions. The microgrid includes a low voltage (LV) distribution system with distributing energy resources (DER) (fuel cells, micro turbines, photovoltaic, etc.) storage devices (energy capacitors and batteries) as well as flexible loads.

Distributed energy resources are a new approach in power system, particularly in Microgrid. Fuel cell converts the chemical energy of the fuel directly to electricity and can serve as an additional energy for the electric grid.

Types, operation principle and mathematical models of fuel cell are considered in thesis. Proton exchange membrane fuel cell (PEMFC) demonstrates potential for use as distributed generation sources. PEMFC can be placed at any site in a distribution system to achieve the best performance without geographic limitations. PEMFCs are good energy sources to provide reliable power at steady state.

This thesis presents the dynamic model development for PEM fuel cells on MATLAB/SIMULINK. Using the equivalent electrical circuit elements and taking into account the double-layer charging effect and the thermodynamic properties we developed a dynamic model for SR-12 type of PEM fuel cell. Simulation model of SR-12 PEMFC on MATLAB/Simulink is developed according to these dynamic models.

Simulation results show that dynamic properties of PEMFC depend on characteristic blocks within FC. The models can predict the electrical response of the PEM fuel-cell stack under steady state as well as transient conditions. The model forecasts the temperature response of the fuel-cell stack, improves the external potential to be used in a controller for PEMFC.

We are going to implement the following to improve the model in our future works:

- Develop detailed fuel cell stack model with load variations.
- Develop hybrid microgrid system of Karabuk University campus consisting of PV panel, energy storage device, fuel cell and loads.
- Consider hybrid microgrid operating modes, in both microgrid connected and disconnected to main grid.

## REFERENCES

1. Carrette,L., Friedrich, K., andStimming, U., "Fuel cells–fundamentals and applications," *Fuel cells*, vol. 1, pp. 5-39, (2001).
2. Rodríguez,C.M.B.,Paleta,M., Marquezv,J., andDelavega, J. R. G., "Effect of a rigid gas diffusion media applied as distributor of reagents in a PEMFC in operation, part II: wet gases," *Int. J. Electrochem. Sci*, vol. 5, pp. 414-428, (2010).
3. Ceraolo,M., Miulli, C., and Pozio,A., "Modelling static and dynamic behaviour of proton exchange membrane fuel cells on the basis of electro-chemical description," *Journal of power sources*, vol. 113, pp. 131-144, (2003).
4. Youssef,M., Nadi, K., and Khalil,M. H., "Lumped model for proton exchange membrane fuel cell (PEMFC)," *International Journal of Electrochemical Science*, vol. 5, pp. 267-277, (2010).
5. Zawodzinski,T.A., Derouin,C.,Radzinski,S., Sherman,R. J., Smith,V.T., Springer,T. E., et al., "Water uptake by and transport through Nafion® 117 membranes," *Journal of the electrochemical society*, vol. 140, pp. 1041-1047, (1993).
6. Junsheng , J., and Xueying,C., "Adaptive Control of MPPT for Fuel Cell Power System," *Journal of Convergence Information Technology*, vol. 8, (2013).
7. Zhong, Z.d., Huo, H.b., Zhu, X.j., Cao, G.y., and Ren,Y., "Adaptive maximum power point tracking control of fuel cell power plants," *Journal of Power Sources*, vol. 176, pp. 259-269, (2008).
8. Karami,N., ElKhoury,L., Khoury,G., and Moubayed,N., "Comparative study between P&O and incremental conductance for fuel cell MPPT," *in Renewable Energies for Developing Countries (REDEC),2014 International Conference on*, pp. 17-22, (2014).
9. Wang,M.-H., Yau,H.-T., and Wang,T.-Y., "Extension sliding mode controller for maximum power point tracking of hydrogen fuel cells," *in Abstract and Applied Analysis*, pp 1-5 (2013).
10. Lu, J., andZahedi, A., "Maximum efficiency point tracking control for fuel cell power systems," *in Power System Technology (POWERCON), 2010 International Conference on*, , pp. 1-6 (2010).

11. Dargahi,M., Rezanejad,M., Rouhi, J., and Shakeri,M., "Maximum power point tracking for fuel cell in fuel cell/battery hybrid systems," *in Multitopic Conference, 2008. INMIC 2008. IEEE International*, pp. 33-37 (2008).
12. Carreon-Bautista,S.,Erbay, C., Han,A., and Sanchez-Sinencio,E., "An Inductorless DC–DC Converter for an Energy Aware Power Management Unit Aimed at Microbial Fuel Cell Arrays," *IEEE Journal of Emerging and Selected Topics in Power Electronics*, vol. 3, pp. 1109-1121, (2015).
13. Ellabban,O., Abu-Rub,H., and Blaabjerg,F., "Renewable energy resources: Current status, future prospects and their enabling technology," *Renewable and Sustainable Energy Reviews*, vol. 39, pp. 748-764, (2014).
14. Bazilian,M., Onyeji,I., Liebreich,M., MacGill,I., Chase,J., Shah, J., et al., "Re-considering the economics of photovoltaic power," *Renewable Energy*, vol. 53, pp. 329-338, (2013).
15. Feldman,D., Barbose, G., Margolis,R., James, T., Weaver,S., Darghouth,N., et al., "Photovoltaic System Pricing Trends: Historical, Recent, and Near-Term Projections. 2014 Edition," *Presentation by SunShot, US Department of Energy*, NREL/PR-6A20-62558, (2014).
16. Sustainable,A., Outlook,E., and Teske,L.S., "Global Wind Energy Council," (2013).
17. Walwyn, D.R., and Brent,A.C., "Renewable energy gathers steam in South Africa," *Renewable and Sustainable Energy Reviews*, vol. 41, pp. 390-401, (2015).
18. Crettenand,N., "The Facilitation of Mini and Small Hydropower in Switzerland: Shaping the Institutional Framework (with a Particular Focus on Storage and Pumped-Storage Schemes)," *Citeseer*,(2012).
19. America, L.A., "*World Small Hydropower Development Report 2013*"(2013).
20. Anup,G., Ian,B., and Sang-Eun,O., "Micro-hydropower: A promising decentralized renewable technology and its impact on rural livelihoods," *Scientific Research and Essays*, vol. 6, pp. 1240-1248, (2011).
21. Ellamla, H.R., Staffell, I., Bujlo,P.,Pollet, B.G., and Pasupathi,S., "Current status of fuel cell based combined heat and power systems for residential sector," *Journal of Power Sources*, vol. 293, pp. 312-328, (2015).
22. Notter, D.A., Kouravelou,K., Karachalios,T., Daletou,M.K., and Haberland, N.T., "Life cycle assessment of PEM FC applications: electric mobility and  $\mu$ -CHP," *Energy & Environmental Science*, vol. 8, pp. 1969-1985, (2015).
23. Ehsani,M., Gao, Y., and Emadi,A., "Modern electric, hybrid electric, and fuel cell vehicles: fundamentals, theory, and design" *CRC press*,(2009).
24. Haile, S.M., "Fuel cell materials and components," *Acta Materialia*, vol. 51, pp. 5981-6000, (2003).

25. Winter M., and Brodd, R.J., "What are batteries, fuel cells, and supercapacitors?," ed: *ACS Publications*,(2004).
26. Larminie, J., Dicks,A., and Donald, M.S., "Fuel cell systems explained vol. 2," *J. Wiley Chichester, UK*,(2003).
27. Williams,M.C., Strakey,J.P., and Surdoval, W.A., "The US department of energy, office of fossil energy stationary fuel cell program," *Journal of Power Sources*, vol. 143, pp. 191-196, (2005).
28. Handbook, F.C., "EG&G technical services," **Inc., Albuquerque, NM**, DOE/NETL-2004/1206,(2004).
29. Steele , B.C., and Heinzl,A., "Materials for fuel-cell technologies," *Nature*, vol. 414, pp. 345-352, (2001).
30. Oh, S., and Logan, B.E., "Hydrogen and electricity production from a food processing wastewater using fermentation and microbial fuel cell technologies," *Water research*, vol. 39, pp. 4673-4682, (2005).
31. Lukas, M.D., Lee, K.Y., andGhezel-Ayagh, H., "Development of a stack simulation model for control study on direct reforming molten carbonate fuel cell power plant," *IEEE Transactions on Energy Conversion*, vol. 14, pp. 1651-1657, (1999).
32. Jaouen,F., Proietti,E., Lefèvre,M., Chenitz,R., Dodelet,J.-P., Wu,G., et al., "Recent advances in non-precious metal catalysis for oxygen-reduction reaction in polymer electrolyte fuel cells," *Energy & Environmental Science*, vol. 4, pp. 114-130, (2011).
33. Pasaogullari,U., and Wang,C., "Liquid water transport in gas diffusion layer of polymer electrolyte fuel cells," *Journal of the Electrochemical Society*, vol. 151, pp. A399-A406, (2004).
34. Krewitt W., and Schmid,S., "Fuel cell technologies and hydrogen production/distribution options," *EU-Project CASCADE Mints. Deutsches Zentrum fur Luft-und Raumfahrt*, Stuttgart, (2005).
35. Diepenhorst,T., Lin,R., Sedik, A.M., Song,T., andSotsky, J., "Fuel Cell Air Intake System," (2009).
36. Choi,W., Howze, J.W. , and Enjeti,P., "Development of an equivalent circuit model of a fuel cell to evaluate the effects of inverter ripple current," *Journal of Power Sources*, vol. 158, pp. 1324-1332, (2006).
37. Wang,C.,Nehrir, M.H., and Shaw, S.R., "Dynamic models and model validation for PEM fuel cells using electrical circuits," *IEEE transactions on energy conversion*, vol. 20, pp. 442-451, 2005.

38. Mehemet, F.K., 'Hydrogen fuel cell powerd electri vhehices and an application of improvement for the desorption efficiency of ametal hydide storage" *istanbultechnicaluniversity*, (2011).
39. Ortum, K.G., *Treatise on Electrochemistry, Elsevier, Amsterdam*, (1965).



## **RESUME**

Muner A. Abdalrazg Khairalla was born in Derna (Libya) in 1987 and he graduated first and elementary education in this city. He completed high school education in Derna High School, after that, he started undergraduate program in Derna The Higher Institute , Department of Electronics Engineering/Derna in 2009 . From 2014 until 2017 he graduated master science education at Karabuk University Department of Electric Electronics Engineering.

### **CONTACT INFORMATION**

Address: Derna / Libya.

Phone: +905452314937, +218927881339

Email: malaokly@yahoo.com